



Pharmaco-electroencephalographic responses in the rat differ between active and inactive locomotor states

Ingeborg H. Hansen^{1,2}  | Claus Agerskov¹  | Lars Arvastson¹ | Jesper F. Bastlund¹ | Helge B. D. Sørensen² | Kjartan F. Herrik¹

¹H. Lundbeck A/S, Valby, Denmark

²DTU Elektro (Technical University of Denmark), Lyngby, Denmark

Correspondence

Ingeborg H. Hansen, H. Lundbeck A/S, Valby, Denmark.

Email: inhe@lundbeck.com

Abstract

Quantitative electroencephalography from freely moving rats is commonly used as a translational tool for predicting drug-effects in humans. We hypothesized that drug-effects may be expressed differently depending on whether the rat is in active locomotion or sitting still during recording sessions, and proposed automatic state-detection as a viable tool for estimating drug-effects free of hypo-/hyperlocomotion-induced effects. We aimed at developing a fully automatic and validated method for detecting two behavioural states: active and inactive, in one-second intervals and to use the method for evaluating ketamine, DOI, d-cycloserine, d-amphetamine, and diazepam effects specifically within each state. The developed state-detector attained high precision with more than 90% of the detected time correctly classified, and multiple differences between the two detected states were discovered. Ketamine-induced delta activity was found specifically related to locomotion. Ketamine and DOI suppressed theta and beta oscillations exclusively during inactivity. Characteristic gamma and high-frequency oscillations (HFO) enhancements of the NMDAR and 5HT_{2A} modulators, speculated associated with locomotion, were profound and often largest during the inactive state. State-specific analyses, theoretically eliminating biases from altered occurrence of locomotion, revealed only few effects of d-amphetamine and diazepam. Overall, drug-effects were most abundant in the inactive state. In conclusion, this new validated and automatic locomotion state-detection method enables fast and reliable state-specific analysis facilitating discovery of state-dependent drug-effects and control for altered occurrence of locomotion. This may ultimately lead to better cross-species translation of electrophysiological effects of pharmacological modulations.

KEYWORDS

amphetamine, d-cycloserine, diazepam, DOI, ketamine

Abbreviations: 5-HT_{2A}, 5-hydroxy-tryptamine_{2A}; Amp, d-amphetamine; AP, Anterior-posterior; DCS, D-cycloserine; Dia, Diazepam; DOI, 2,5-Dimethoxy-4-iodoamphetamine; DV, Dorsal-ventral; ECoG, Electrocorticogram; EEG, Electroencephalogram; HFO, High-frequency oscillations; Ket, Ketamine; LFP, Local field potentials; ML, Medial-lateral; mPFC, Medial prefrontal cortex; NMDAR, N-methyl-D-aspartate receptors; PCP, Phencyclidine; PPV, Positive predictive value; SC, Subcutaneous; TPR, True positive rate.

Edited by Prof. Jochen Roeper. Reviewed by Mariana Barassi and Wilhelmus Drinkenburg.

All peer review communications can be found with the online version of the article.

This is an open access article under the terms of the Creative Commons Attribution-NonCommercial-NoDerivs License, which permits use and distribution in any medium, provided the original work is properly cited, the use is non-commercial and no modifications or adaptations are made.

© 2019 The Authors. *European Journal of Neuroscience* published by Federation of European Neuroscience Societies and John Wiley & Sons Ltd.

1 | INTRODUCTION

In drug development, a widely used cross-species translational tool for predicting the clinical effect of pharmacological compounds is to assess effects on brain activity by measuring electrocorticograms (ECoGs) and local field potentials (LFPs) from the rat brain during free and spontaneous behaviour. The predictive validity of such animal studies depends on controlling several factors in the experimental design affecting the translational value (Denayer, Stöhr, & van Roy, 2017). In clinical resting state studies, human subjects sit quietly to standardize recording conditions and prevent movement artefacts (Jobert et al., 2012) while rats often are allowed to move freely about the recording arena to enable natural behaviour and to avoid stressing the animals (Kislin et al., 2014; Lee, Shtengel, Osborne, & Lee, 2014; Schwarz et al., 2010). Differences in motor activity may impede translation of research findings between species and pharmac-EEG studies in animals may produce discrepant results due to movement-related changes in LFP/ECoG. In this study, we show that oscillatory activity in the delta to high frequency bands (0.1–200 Hz) differs between active and inactive behaviours, and that the state of the animal may determine the sensitivity of ECoG/LFP recordings to pharmacologically induced changes in oscillatory activity. Hyperlocomotion-related effects on ECoG/LFP can i.a. be expected in animal pharmac-EEG studies investigating models of NMDAR hypofunction (Goff, 2017), since commonly used non-competitive NMDAR antagonists, such as ketamine, may induce hyperlocomotion in rodents (Caixeta, Cornélio, Scheffer-Teixeira, Ribeiro, & Tort, 2013; Hunt, Raynaud, & Garcia, 2006; Imre, Fokkema, Den Boer, & Ter Horst, 2006; Matulewicz, Kasicki, & Hunt, 2010; Nicolás et al., 2011; Páleníček et al., 2011). In contemporary schizophrenia research, neuronal oscillations have received much attention. Non-competitive NMDAR antagonists increase gamma while antipsychotics reduce both gamma and locomotor activity (Ahnaou, Huysmans, van de Castele, & Drinkenburg, 2017), however, findings that ketamine-induced gamma (Hakami et al., 2009; Nicolás et al., 2011) and HFO (Hunt et al., 2006; Lee, Hudson, O'Brien, Nithianantharajah, & Jones, 2017) correlate with the level of locomotor activity have demonstrated the need to determine whether changes in ECoG/LFP simply reflect drug-induced hyperlocomotion or not. In support for a locomotion-independent effect on gamma oscillations, Hakami et al. (2009) found that ketamine enhances gamma activity in different brain states of sedation. However, ketamine induced increases in HFO are prevented by anaesthesia (Amat-Foraster et al., 2018; Hunt, Matulewicz, Gottesmann, & Kasicki, 2009). In the awake state, drug-effects on LFP/ECoG evaluated specifically within a behavioural state have most often been obtained through manual behavioural scoring (Coenen & van Luijtelaa, 1989; Leccese, Marquis, Mattia, & Moreton, 1986; Sławińska & Kasicki,

1998; van Lier, Drinkenburg, van Eeten, & Coenen, 2004), which is tedious and time-consuming work possibly prone to varying detection-precision. Although technical solutions to track locomotor activity in rodents have been used for long (Schmitt & Hiemke, 1998), and behavioural-state classification methods have been developed and validated against manual scoring (Belic, Halje, Richter, Petersson, & Kotaleski, 2015; Dollar, Rabaud, Garrison, & Belongie, 2005; Farah, Langlois, & Bilodeau, 2016; Jhuang et al., 2010; Steele, Jackson, King, & Lindquist, 2007; van Dam et al., 2013; Zarringhalam et al., 2012) we have found that studies, analysing LFP/ECoG in specific automatically detected states, use methods unvalidated against manual scoring (Ahnaou, Huysmans, Biermans, Manyakov, & Drinkenburg, 2017; Ahnaou, Huysmans, van de Castele, et al., 2017; Kealy, Commins, & Lowry, 2017; Lee et al., 2017). How well behaviour is classified inevitably determines the reliability of subsequent state-specific analyses, thus employing methods with high classification performance and time-resolution is important. Alternative approaches include fixing the head of the rodent while recording rotation of a subjacent spherical treadmill (Ayaz, Saleem, Schölvink, & Carandini, 2013; Keller, Bonhoeffer, & Hübener, 2012; Niell & Stryker, 2010) and training rats to walk on a circular treadmill during recording (Furth et al., 2017). In this study, we investigated awake rats allowed natural and spontaneous behaviour and detected periods of inactivity and locomotion automatically in 1-second epochs using a validated method enabling state-specific evaluation of drug-effects. A range of drugs targeting different neurotransmitter systems and expected to exert differential effects on locomotion and ECoG/LFP were investigated: NMDAR antagonist ketamine; d-cycloserine classified as a NMDAR glycine site partial agonist (Hood, Compton, & Monahan, 1989) with antagonist effects predominating at high doses (Goff, 2017; Heresco-Levy et al., 2013); the hallucinogen and 5-HT_{2A}-agonist, 2,5-Dimethoxy-4-iodoamphetamine (DOI); the locomotor stimulant d-amphetamine; and the locomotor depressant diazepam. The aim of the study was to enable more detailed and accurate estimation of drug effects by minimizing effects caused by changed occurrence of locomotion and by providing knowledge on how drug-effects are expressed specifically during inactivity and locomotion.

2 | MATERIALS AND METHODS

Two datasets were obtained (a) for the development of a locomotive-state detector ($N = 32$ rats) and (b) for assessing effects of pharmacological compounds in the inactive and the active state, specifically ($N = 50$ rats). Male Wistar rats (Charles River, Germany), were housed in cages with sawdust bedding and environmental enrichment (plastic house, wooden chew blocks, and paper bedding material) with ad libitum access to

chow and water in environmentally controlled conditions with a 12:12 hr reversed light:dark cycle (lights off at 6:00 AM).

Experimental procedures and animal housing and care were carried out in accordance with the Danish legislation according to the European Union regulation (directive 2010/63 of 22 September 2010), granted by the Animal Welfare Committee, appointed by the Ministry of Environment and Food of Denmark.

2.1 | Drugs

(R,S)-Ketamine (Ketolar 50 mg/ml, Pfizer), hereafter ketamine at 3, 10, and 30 mg/kg, d-cycloserine (synthesized at Lundbeck) at doses 100 and 300 mg/kg, 2,5-Dimethoxy-4-iodoamphetamine (DOI) (Sigma-Aldrich) at 1 mg/kg, d-amphetamine (Sigma-Aldrich) at 1 mg/kg, and diazepam (Sigma-Aldrich) at 1 mg/kg were dissolved in 0.9% saline (5 ml/kg). Control animals received 0.9% saline. All drugs and vehicles (veh) were administered subcutaneously (s.c.) after a + 120 min habituation period of which the last 30 min served as a baseline recording. Doses of amphetamine, diazepam, and DOI were selected based on previous studies showing influence on neural oscillations and/or locomotor activity (Coenen & van Luijtelaa, 1989; Goda, Piasecka, Olszewski, Kasicki, & Hunt, 2013; Krijzer, Koopman, & Olivier, 1993).

2.2 | Surgical procedure

On the day of surgery, rats (270–300 g) were anaesthetized with a 0.25 ml/100 g subcutaneous (SC) injection of 1:1 hypnorm/Dormicum and mounted in a stereotaxic frame (David Kopf Instruments, Tujunga, CA, USA) with blunt ear bars. Marcain (0.2 ml SC) was injected under the scalp, and gel (Neutral Ophtha Eye Gel) put on the eyes to prevent the mucous membrane drying out. Holes were burred in the skull to allow for placement of two depth electrodes (E363-series; PlasticsOne, Roanoke, VA, USA) in left and right pre/infralimbic PFC (AP: 3.0 mm from the bregma suture, ML: \pm 0.7 mm from the sagittal suture and DV: 3.0 mm from the dura) and thalamus (AP: $-$ 2.8 mm from the bregma suture, ML: +0.7 mm from the sagittal suture and DV: 4.4 mm from the dura) and three screw electrodes at vertex (AP: $-$ 2 mm from the bregma suture, ML: +2.0 mm from the sagittal suture), a reference electrode (AP: +8.0 mm and ML: $-$ 2.0 mm), and a ground electrode (AP: $-$ 5 mm, ML: +5 mm). During surgeries, nails were cut to prevent rats from scratching wounds following surgery. After completion of surgeries, rats were placed under warming lamps until recovery of consciousness (maximum 4 hr). Water-soaked food pellets were placed in the home cage so the rat easily and quickly could start feeding. Extra muesli was supplied to aid the recovery. Rats were treated with Norodyl and Noromox for 5 days in total and closely observed during

a 10–14-day post-surgery recovery period. Animal bodyweights were recorded daily. No rats lost more than 10% of their pre-surgery bodyweight. Sutures were removed after 7–10 days. At the end of experiments electrical lesions were performed in all recording electrodes and brains were cut for visual microscopy inspection of electrode placement. The differences between depth- and screw-electrode impedances were handled by investigating relative power changes and common-mode noise sources were reduced from recording in shielded boxes and excluding power estimates around 50, 100, and 150 Hz from analyses.

2.3 | Electrophysiological recordings

Rats were handled daily and habituated to recording box the week before recording sessions. Recordings were performed during the dark phase of the light/dark cycle. At 8 AM, rats (400–500 g) were individually transferred to an acrylic chamber (30 cm wide 45 cm deep 55 cm high) placed within an electrically shielded sound-proof box (90 cm wide 55 cm deep 65 cm high) and were tethered to a six-pin wire suspended from a rotating swivel, allowing free movement within the recording box. Rats used for the first dataset were habituated for 1 hr and subsequently scored in 10–15 min to have both activity and inactivity well represented. For the second dataset, there was a 2-hr habituation period followed by 45 min of baseline recording, whereafter rats were injected subcutaneously with vehicles or vehicle + compound and left in the box for two more hours. Rats only went through recording sessions once a week with at least 6 days between recordings to allow for wash-out of compounds. The analog LFP/ECoG signals were amplified and band-pass filtered at 0.01–300 Hz (Precision Model 440; Brownlee, Palo Alto, CA, USA) and converted to a digital signal at a sampling rate of 1 kHz (CED Power 1401, Power 1 (625 kHz, 16 bit) and CED Expansion ADC16; CED, Cambridge, England). An analog 50 Hz notch filter (Precision Model 440, Brownlee) was applied to the LFP/ECoG signals of the first dataset, but was not applied in the following pharmaco-EEG experiments. Video recordings were processed in EthoVision producing the mobility signal, which was subsequently collected in Spike2 along with the LFP/ECoG signals with a delay used subsequently to synchronize the signals.

2.4 | Data analysis

The development of the locomotive state-detection algorithm and the state-specific pharmaco-EEG analyses were carried out in MATLAB R2017a (The MathWorks, Inc., Natick, MA, USA) using functions from the sigTOOL toolbox (Lidierth, 2009; <https://sourceforge.net/projects/sigtool/>).

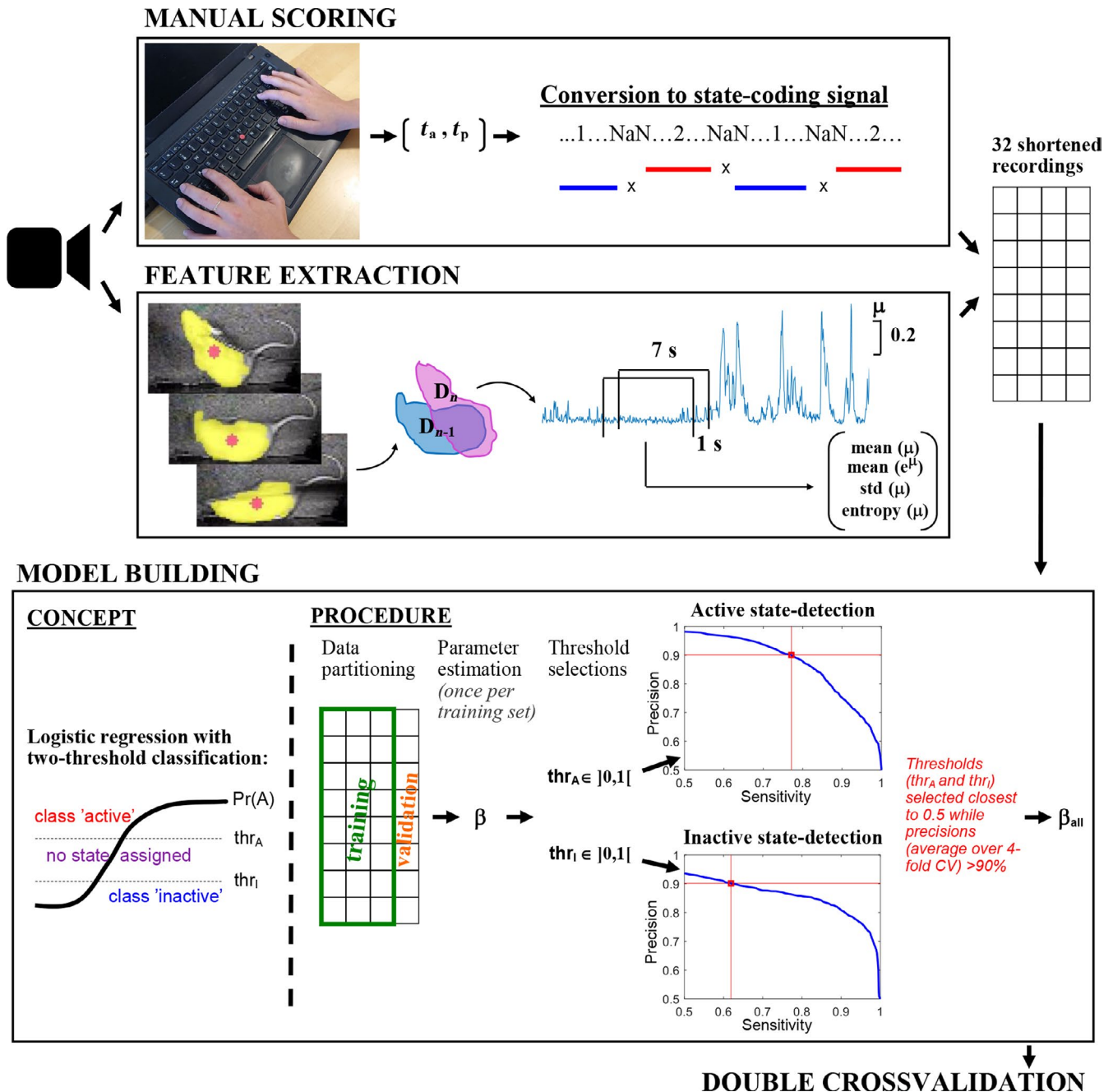


FIGURE 1 Schematic showing the steps of the development of the locomotive state detection algorithm. Video recording of rats was used to obtain labelled data from manual scoring as well as a mobility signal using EthoVision XT. Labelled data were obtained by having an experienced technician mark the times of state-change, t_a and t_p , through time-registered keyboard presses. The times of state-change were converted to a continuous discrete signal coding for behaviour where 1-s before each registration of state-change was marked with NaN-values to exclude uncertain transition periods in the subsequent training of the classifier. The developed state-detection algorithm was based on features of the mobility signal, μ , obtained with EthoVision software which reflected the change in the detected (yellow) area of the rat over video-frames. A range of features of μ were calculated in windows of 7 s moving in steps of 1 s, and four features were selected for use in the classification. The 32 recordings (manual scoring and feature signals) were shortened to have equal representation of both states before training the classifier. The probability for active state, $\text{Pr}(A)$, (and implicitly inactive state) given the features was predicted using binomial logistic regression, and two probability-thresholds, thr_A and thr_I , were used to assign samples to the active state when $\text{Pr}(A) > \text{thr}_A$ and the inactive state when $\text{Pr}(A) < \text{thr}_I$. Thresholds were selected by sweeping through values from zero to one in steps of 0.01 and subsequently choosing thr_A - and thr_I -values closest to 0.5 for which the resultant state-detection precisions (based on fourfold cross-validation) were above 90%. Finally, the logistic regression parameters were estimated based on all 32 recordings. The classification performance of the whole model building procedure was tested using double-cross-validation. [Colour figure can be viewed at wileyonlinelibrary.com]

2.4.1 | Development of the locomotive state detection algorithm

A classification algorithm was made for detecting periods during which the rat was in either of two states: active and inactive state (Figure 1). The active state was defined by both horizontal and vertical locomotion including walking, running, and rearing, while the inactive state was defined by no locomotion including immobility, grooming, and sniffing behaviours scored on-line by an experienced technician marking times for state-change by pressing “a” and “p” on a keyboard sampled at a 25 Hz rate. The state-detection was based on features of a mobility signal of 25 Hz sampling rate obtained using the tracking system EthoVision XT v7 from Noldus Information Technology. The mobility signal is based on video recordings of the rats and reflects the changes in the rat detection in one frame, D_n , compared with the previous D_{n-1} (illustrated in Figure 1a) as described by Equation 1, where $Area(\cdot)$ signifies the area of a set, that is, a pixel count.

$$\mu_n = \frac{Area(D_n \cup D_{n-1}) / D_n \cap D_{n-1}}{Area(D_n) + Area(D_{n-1})}$$

Feature selection was done by investigating a range of measures extracted from the mobility signal in windows of 1, 7, 9, and 15 s moving along the signal in 1-s-steps. Guided by the Fisher ratio class separability measure (Duda and Hart, 1973), a final set of four features based on μ were selected: Shannon entropy, standard deviation, mean, mean (e^μ); and calculated on moving windows of 7 s, comprising a small but synergetic set of features. The entropy feature may enhance the joint class separability particularly in the case when problematic flickering between correct and false detections of the rat area occurs during inactivity. For each of 32 recordings, feature-signals were shortened to ensure exact equal representation of active and inactive state. The classifier was built by predicting probabilities for the two locomotive states for every second based on the four features using logistic regression selected due to probabilistic output and the well-known easy interpretation properties (as opposed to, e.g., non-linear classifiers like support-vector-machine or random forests). Instead of having one decision boundary between the two classes at 50% probability for each state, two probability thresholds were used, leaving periods with probabilities closer to 50% unassigned. This was done to prioritize high precision (i.e., a high proportion of the detected periods being correctly classified) at the expense of sensitivity. The value of each threshold was selected to be as close to 50% while ensuring that > 90% of the resultant classifications were correct. This was done by sweeping through threshold values from zero to one in steps of 0.01 and (for each value) evaluating

the classification performance (Figure 1) as an average fourfold cross-validation (logistic regression model trained on 24 recordings and tested on eight). Test and training sets used in the cross-validation contained whole recordings to avoid potential similarities in data from the same recording biasing performance measures, and fourfold partitioning was chosen (instead of e.g., leave-one-out) due to some recordings containing only little data after shortening to obtain equal representation of the two states. Performance measures were calculated after marking detections shorter than 2 s as unassigned to properly reflect the state-detections used for subsequent spectral analysis of the LFP/ECOG recordings. The state-detections were done on a one-second basis to allow detected state-changes to occur closer to the “true” state changes. After selecting the thresholds, the coefficients for the logistic model were estimated from all recordings to base the model on as much empirical data as possible.

2.4.2 | Cross-validating performance of the locomotive-state detection

Double cross-validation was used to test the performance of the whole procedure described above on “first seen” data. The outer cross-validation loop was run over an eightfold partitioning of data leaving 28 recordings in the training set to be used in the inner loop for building and selecting the best classifier using the procedure described above. The eightfold partitioning of the outer cross-validation loop was chosen to allow fourfold cross-validation on whole recordings in the inner loop, and to have low bias relative to the final detection method developed on all recordings.

2.4.3 | Preprocessing of field potentials

The field potential recordings were preprocessed to enable state-specific spectral analysis of the recordings after drug injection relative to baseline. Initially, the recording files were read into MATLAB using sigTOOL, and field potential recordings were split into 10 min segments to reduce processing load. The last 20 min before injection were not included in the analysis due to possible agitation of the animals while technician worked near the recording stations. As recording stations were shielded, no off-line filtering was done. For the artefact rejection, the following threshold τ was calculated for each segment, separately for each animal:

$$\tau = \max(\bar{\mathbf{S}} + 2\sigma_{\mathbf{S}})$$

where $\bar{\mathbf{S}}$ is a vector containing the signal mean of each channel and $\sigma_{\mathbf{S}}$ is a vector containing the standard deviation of the signal in those channels. The maximum value is then evaluated across the channels. Finally, a mean threshold $\bar{\tau}$ is

obtained for each animal by calculating the average threshold over all 10 min segments. Each sample in every recording channel is then compared to \bar{z} , and if a sample is found to be above, it is labelled as an artefact and removed from further analysis, along with 100 ms of signal before and after the sample. Finally, non-artefacted signal recorded during either locomotion or inactivity, as detected by the state-detection algorithm, was identified and segments of 2 s or more were extracted.

2.4.4 | Spectral analysis

The spectral analysis served to quantify the drug-induced changes of oscillatory activities in signal segments recorded during locomotion and inactivity, separately, as well as on the total data (with artefacts removed). Power spectral density estimates were obtained using Welch's method (Hayes, 1996) with 2 s windows leading to a frequency resolution of ~ 0.5 Hz. Hamming windowing and 50% overlap were applied. Drug-induced changes in power spectra were evaluated relative to baseline (30–20 min before injection) within each animal and electrode, and for the state-specific analyses both the post-injection and baseline data were acquired specifically within a locomotive state.

2.5 | Statistical analyses

The hypotheses tested in the study were related to the usefulness of the automatic locomotive state (LS) detector as well as to the effects of the investigated drugs and locomotive states on oscillatory activity. Two types of response variables were investigated in the statistical analyses: the average power in six frequency bands of the power spectra: delta (1–4 Hz), theta (4–10 Hz), beta (10–30 Hz), low gamma (30–60 Hz), high gamma (60–100 Hz), and HFO (130–160 Hz); as well as the time spent in active/inactive state. The average powers were not affected by any power line noise, since sections of the power spectra of 2 Hz width centred at 50, 100, and 150 Hz were excluded.

Whether the automatic LS detector was a suitable replacement for manual LS scoring was evaluated by testing whether the average powers obtained for active/inactive state was different for the automatic LS scoring as compared to the manual. On the same dataset and for both scoring methods, it was tested whether locomotion affected the average powers by comparing active state with the inactive. Both tests were performed by log-transforming the average powers to obtain normality and differences were tested using paired-sample *t*-testing. Correction for multiple test was done using the Benjamini & Hochberg false-discovery-rate (FDR) correction for multiple tests and a false discovery rate of 5% was used as the significance criterion.

A second dataset was used to test whether the injected drugs had different effects on the average powers (of baseline normalized power spectra) than saline and whether the impact of the drugs was different for the two locomotive states. Statistical mixed effects modelling was used to handle dependencies between observations acquired from the same rat over time, locomotive states, and over a subset of the investigated drugs. Subject-specific intercepts were allowed as random effects and an unstructured correlation matrix was assumed. For each frequency band and brain region, a mixed effects model was fitted to log-transformed power estimates using the backward variable elimination strategy (Hocking, 1976) starting with the full model involving all explanatory variables: “drug dose injected,” “time-interval after injection,” “locomotive state”; and their interactions. An alpha level of 5% was used as the significance criterion, and correction for multiple tests was done for each frequency and brain region as part of the post-hoc testing using the Tukey-Kramer method. Significant differences at specific time-intervals were only presented when relevant interactions with time were significant.

On the same dataset, the effects of the injected drugs on the time spent in active/inactive state as compared to saline was evaluated using the same kind of mixed effects model as described above, however, the model variables were predetermined and included “drug dose injected,” “time-interval after injection,” and their interaction. All statistical analyses were performed using MATLAB 2017a.

3 | RESULTS

In this study, we used LFP and ECoG signals from freely moving rats in combination with locomotion tracking to investigate effects of pharmacological interventions on oscillatory activity separately in two states: an active state of locomotion including horizontal movement and rearings and an inactive state defined by no locomotion of the body. To enable these analyses, an automatic locomotive-state detection algorithm was developed and validated against manual scorings.

3.1 | Locomotive state classification-algorithm detects states of activity and inactivity

The locomotive state detection method, designed to obtain high precision at the expense of sensitivity, detected periods in active and inactive states with 91% and 100% of the detected time correctly classified while sensitivities were 76% and 74%, respectively, and 21% of data was marked unassigned as estimated on “first seen” data using the double cross-validation (Table 1). Performance metrics were

calculated after marking detections too short for spectral analysis of LFP/ECoGs (<2 s) as “unassigned,” to reflect classification quality on data used in subsequent analyses, and changed only up to 1 percentage point if keeping detections of 1 s duration in. The automatic classifier detected 3.1 ± 0.5 min active state and 2.6 ± 0.4 min inactive state in each recording containing 3.5 ± 0.5 min of each state in the balanced dataset. The probabilistic thresholds defining active and inactive states based on the output of the logistic regression were $\text{thr}_A = 0.64$ and $\text{thr}_I = 0.23$, respectively, in the final model. Favouring precision in the classification rather than sensitivity allowed for creating a detection algorithm with high reliability of the data selected for each state. Agreement between manual and automatic methods were thus expected also on power spectra of classified recordings, although differences could occur as the manual scorer ascribed periods of indeterminate behaviour to either the active or inactive state, while the automatic detection excluded such periods. Both detection methods produced the same conclusions when statistically evaluating differences between active and inactive state on delta, theta, beta, low gamma, high gamma, and HFO powers except for a minor increase in power of beta oscillations in mPFC found with the manual scoring (Table 2). No differences were found between the

power estimates of the two methods except on six (out of 48) comparisons. Automatically detected inactive state contained more theta power at LFPs. In the automatically detected active state, delta power was higher in right mPFC and lower in the ECoG (as for the locomotion-induced change), and high gamma power was higher at right mPFC.

3.2 | Spectral powers change from inactive state to active state across all frequency bands

Comparison between the power spectra for the active and inactive state showed that the power spectrum is markedly altered during locomotion over most frequency bands both for the manual and automatic scorings (Figure 2b). In all brain regions, the average theta, low gamma, high gamma, and HFO power were increased in the active state as compared to the inactive state (Table 2). Delta power, similarly, was increased during activity in thalamus and mPFC. Contrary in the ECoG, there was a decrease in both delta and beta power during locomotion compared to during inactivity. The slightly increased power in the beta band in mPFC was significant only for the manually scored data. The largest estimates of spectral power changes associated with locomotion were found in the theta band with more than 100% increase relative to inactivity. Increases up to ~90% were observed in the delta and high gamma bands, while increases in the low gamma and HFO bands were in the range 12%–65%.

3.3 | Pharmacological modulation of locomotion

The automatic state-detection was used to assess whether and how locomotor activity was modulated by: ketamine (3, 10, and 30 mg/kg), d-cycloserine (100 and 300 mg/kg), DOI

TABLE 1 Double cross-validated classification performance in percent (average \pm standard deviation)

Perf.\State	Active state	Inactive state
Precision	91.2 \pm 8.2	100.0 \pm 0
Sensitivity	75.5 \pm 15.4	74.4 \pm 15.3
Accuracy	70.9 \pm 6.9	
Unassigned	20.7 \pm 5.9	

TABLE 2 Changes in spectral powers during locomotion. [Colour figure can be viewed at wileyonlinelibrary.com]

(a) Manual						
Ch.\Freq.	δ	θ	β	γ_L	γ_H	HFO
ECoG	58	124	58	149	155	148
Thalam.	120	194		125	151	165
mPFC(r)	186	268	123	156	191	156
mPFC(l)	146	234	132	143	167	114
(b) Automatic						
Ch.\Freq.	δ	θ	β	γ_L	γ_H	HFO
ECoG	53	124	61	148	159	114
Thalam.	130	182		128	155	112
mPFC(r)	196	214		154	197	118
mPFC(l)	144	188		140	174	114

Note. Significant increases (red) and decreases (blue) in spectral power during locomotion compared to during inactivity. Numbers indicate power in the active state relative to power in the inactive state in percent (100% means no change on average).

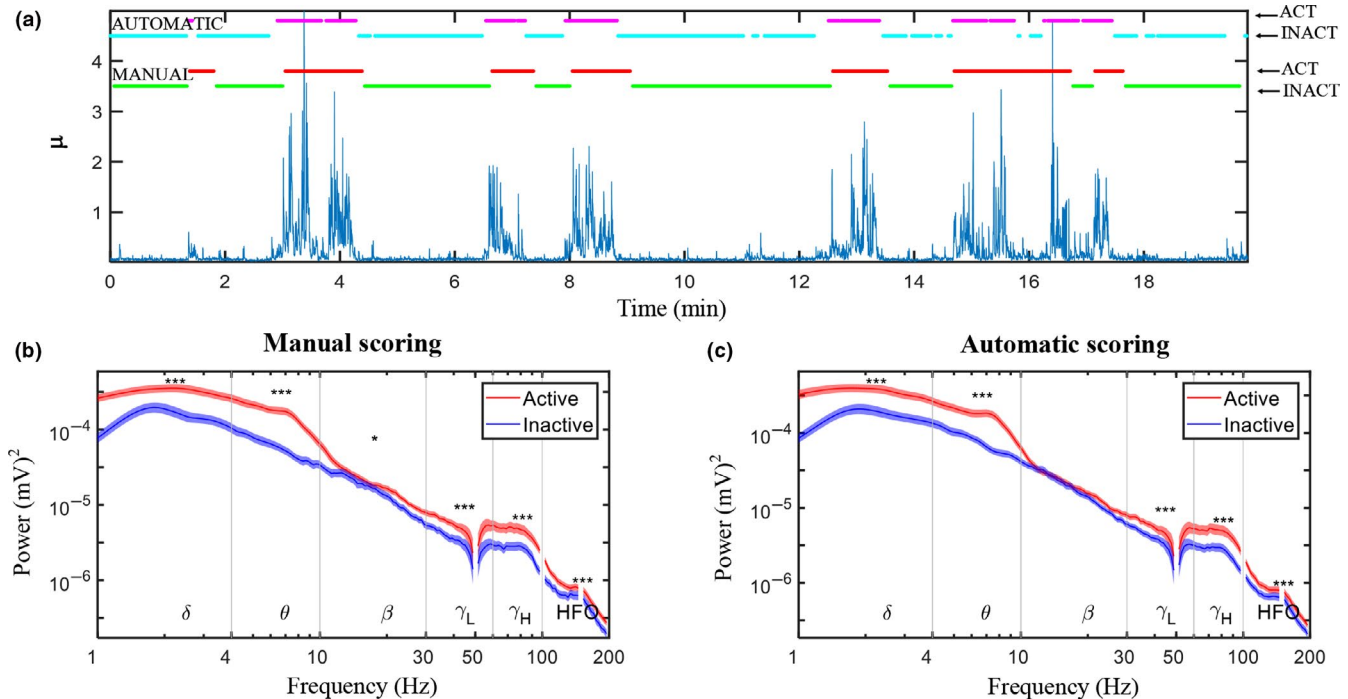


FIGURE 2 (a) Example of the manual scoring (activity and inactive periods shown in red and green, respectively) shown alongside the automatic locomotive state classification (activity and inactive periods shown in purple and light blue, respectively). (b) Power spectra (average over 32 rats from left medial prefrontal cortex) of recordings obtained during active (red graph) and inactive (blue graph) states scored manually (left) and using the automatic LS detection (right). (c) Standard error of the mean (SEM) given as the shaded areas above and below the graphs and significant differences between active and inactive states are marked above the graph when $p < 0.05$ (*), 0.01 (**), and 0.001 (***). [Colour figure can be viewed at wileyonlinelibrary.com]

(1 mg/kg), d-amphetamine (1 mg/kg), and diazepam (1 mg/kg); based on the detected time spent in the active and inactive states within intervals of 10 min. The high dose of ketamine (30 mg/kg) increased the detected time spent in active state and decreased the time spent in inactive state. The 10 mg/kg dose of ketamine produced no changes, while the lowest dose (3 mg/kg) of ketamine decreased the time spent in active state and increased the time spent in inactive state as detected by the algorithm (Figure 3a left column). D-cycloserine, DOI, and diazepam did not induce significant changes in time spent in active or inactive states, whereas amphetamine produced marked increases in time spent in active state 10–120 min after injection compared to the vehicle (Figure 3a). The detected changes in locomotor activity were similar to those found when assessing drug-induced effects based on infrared beam breaks (cf. Supporting Information Figures S1 and S2).

3.4 | Locomotive state-specific modulations of spectral power

The separate evaluation of drug effects within the active and inactive states revealed ubiquitous effects expressed in both states as well as effects occurring exclusively in one state (Tables 3 and 4). The baseline-corrected and state-specific power spectra (examples shown in Figure 3b) showed distinct

and confined drug-induced alterations in the lower frequencies only present in one locomotive state while the curvature of power spectra across higher frequencies were more similar in the two states. Evaluating drug-induced changes as averages within the six frequency bands showed that most of the detected drug-effects differed significantly between the two states (marked by squares in Tables 3 and 4). Specific analyses of the inactive state, enabling the identification of drug-effects on spectral powers not associated with locomotor activity, revealed ketamine-induced changes across the theta, beta, low gamma, high gamma, and HFO bands, d-cycloserine induced changes across the high gamma and HFO bands, DOI induced changes across the delta, theta, beta, and HFO bands, and diazepam-induced changes in the beta band when comparing average power changes to those of vehicle (Table 4). Below is a detailed description of the drug-effects on oscillatory activity as expressed specifically during locomotion and during inactivity relative to the corresponding state-specific baseline estimates.

3.4.1 | Ketamine

Delta activity

Ketamine effects on delta activity in the LFPs showed increases of delta power in the active state emerging early

FIGURE 3 Drug effects on locomotion and LFP power spectra from right medial prefrontal cortex. (a) Effects of ketamine (Ket), d-cycloserine (DCS), DOI, amphetamine (Amp), and diazepam (Dia) on time spent in the active and inactive state (on average over rats) as determined by the automatic LS detector. Standard error of the mean (SEM) given as the shaded areas above and below the graphs. Time-intervals where drug-induced changes differ from saline are marked above the graphs when $p < 0.05$ (*), 0.01 (**), or 0.001 (***) (b) Power spectra based on 10-min time intervals after injection for Ket (30–40 min after), DCS (80–90 min after), and for DOI, Dia, and Amp (70–80 min after) calculated from active state, inactive state, and total data. The power spectra are baseline-corrected and averaged over rats, and shaded areas mark the SEM. (c) Heatplots showing averaged baseline-corrected power spectra during inactivity for each 10-min time interval of the recordings in mPFC_{right} for administrations of the large doses of ketamine and DCS as well as DOI. The two black lines in the heatplots frame in the time-intervals shown in part B. [Colour figure can be viewed at wileyonlinelibrary.com]

after administration (Figure 4). In the inactive state, only tendencies to decrease were observed. The significant increases were induced by the high dose of 30 mg/kg ketamine in right mPFC and thalamus (Table 3) occurring within an interval from 10 to 40 min after administration.

The ECoG did not display ketamine-induced enhancement of delta oscillations. When evaluating the effect of ketamine on the total data not segmented according to locomotive state, ketamine was found to increase delta power in the LFP channels (Table 5).

TABLE 3 Power changes induced by drugs compared to vehicle in active state. [Colour table can be viewed at wileyonlinelibrary.com]

A Left mPFC

Drug\Freq	δ	θ	β	γ_L	γ_H	HFO
Ket 30				212		840
Ket 10						332
Ket 3						
DCS 300						516
DCS 100						145
Dia						
Amp						
DOI						110

B Right mPFC

Drug\Freq	δ	θ	β	γ_L	γ_H	HFO
Ket 30	205			236		673
Ket 10						423
Ket 3						
DCS 300						690
DCS 100						124
Dia						
Amp						
DOI						121

C Thalamus

Drug\Freq	δ	θ	β	γ_L	γ_H	HFO
Ket 30	236			122		465
Ket 10						198
Ket 3						
DCS 300						375
DCS 100						
Dia						
Amp						
DOI						

D ECoG

Drug\Freq	δ	θ	β	γ_L	γ_H	HFO
Ket 30				360	78	476
Ket 10				173		156
Ket 3						
DCS 300						328
DCS 100						107
Dia						
Amp		97				
DOI						

Note. Tables mark pharmacologically induced changes to a frequency band in the active state which was found significantly different than vehicle in one or more time-bins within the 2 hr of recording after injection (12 time bins). Significant increases are marked with red and significant decreases are marked with blue. The numbers within colour-coded cells show the difference between compound and vehicle induced changes from baseline (in percentage points), and only the largest difference found over the 12 time bins is given. The estimated differences between a compound and vehicle are determined based on the log-transformed estimates of the fitted statistical model. Cells marked with thick-lined square indicate that a discovered change from baseline is significantly different to the change elicited in the inactive state.

TABLE 4 Power changes induced by drugs compared to vehicle in inactive state. [Colour table can be viewed at wileyonlinelibrary.com]

A Left mPFC

Drug\Freq	δ	θ	β	γ L	γ H	HFO
Ket 30			55	281	105	1274
Ket 10						531
Ket 3						111
DCS 300					75	1026
DCS 100						202
Dia						
Amp						
DOI						304

B Right mPFC

Drug\Freq	δ	θ	β	γ L	γ H	HFO
Ket 30		93	70	357	98	1329
Ket 10				78		685
Ket 3						
DCS 300					87	1295
DCS 100						154
Dia						
Amp						
DOI		81				278

C Thalamus

Drug\Freq	δ	θ	β	γ L	γ H	HFO
Ket 30		68	70	138	125	929
Ket 10		67	62			400
Ket 3						
DCS 300					85	854
DCS 100						
Dia			85			
Amp						
DOI	93	83	77			244

D ECoG

Drug\Freq	δ	θ	β	γ L	γ H	HFO
Ket 30		63	51	357	133	897
Ket 10		63	51	135	81	354
Ket 3						93
DCS 300					76	717
DCS 100						121
Dia			81			
Amp						
DOI	69	57	56			240

Note. Tables mark pharmacologically induced changes to a frequency band in the inactive state which was found significantly different than vehicle in one or more time bins within the 2 hr of recording after injection (12 time bins). Significant increases are marked with red and significant decreases are marked with blue. The numbers within colour-coded cells show the difference between compound and vehicle induced changes from baseline (in percentage points), and only the largest difference found over the 12 time bins is given. The estimated differences between a compound and vehicle are determined based on the log-transformed estimates of the fitted statistical model. Cells marked with thick-lined square indicate that a discovered change from baseline is significantly different to the change elicited in the active state.

Theta activity

Ketamine suppressed theta powers during the inactive state only and the suppressions were in many cases significantly different to the relative change within the active state (Tables 3 and 4). In the inactive state, the 10 and 30 mg/kg doses of ketamine suppressed theta activity in right mPFC, thalamus and in the ECoG. Significant theta suppressions were found in an interval from 20 min after administration till the end of recording at 120 min after administration. In the total data not segmented according to locomotive state, theta power was decreased in right mPFC and in the ECoG. Significant effects were found in no more than three time bins whereas suppressions evaluated on the inactive state data were more pronounced.

Beta activity

Ketamine suppressed beta powers during the inactive state only and the suppressions were in many cases significantly different to the relative change within the active state (Tables 3 and 4). In the inactive state, the 10 and 30 mg/kg doses of ketamine suppressed beta activity in thalamus and in the ECoG, and the 30 mg/kg dose of ketamine suppressed beta activity in left and right mPFC. Beta suppressions were found consistently in thalamus from right after injection till the end of recording at 120 min after administration. In mPFC and the ECoG, significant effects occurred from 10 to 90 min after administration, respectively. In the total data not segmented according to locomotive state, beta power was decreased in right

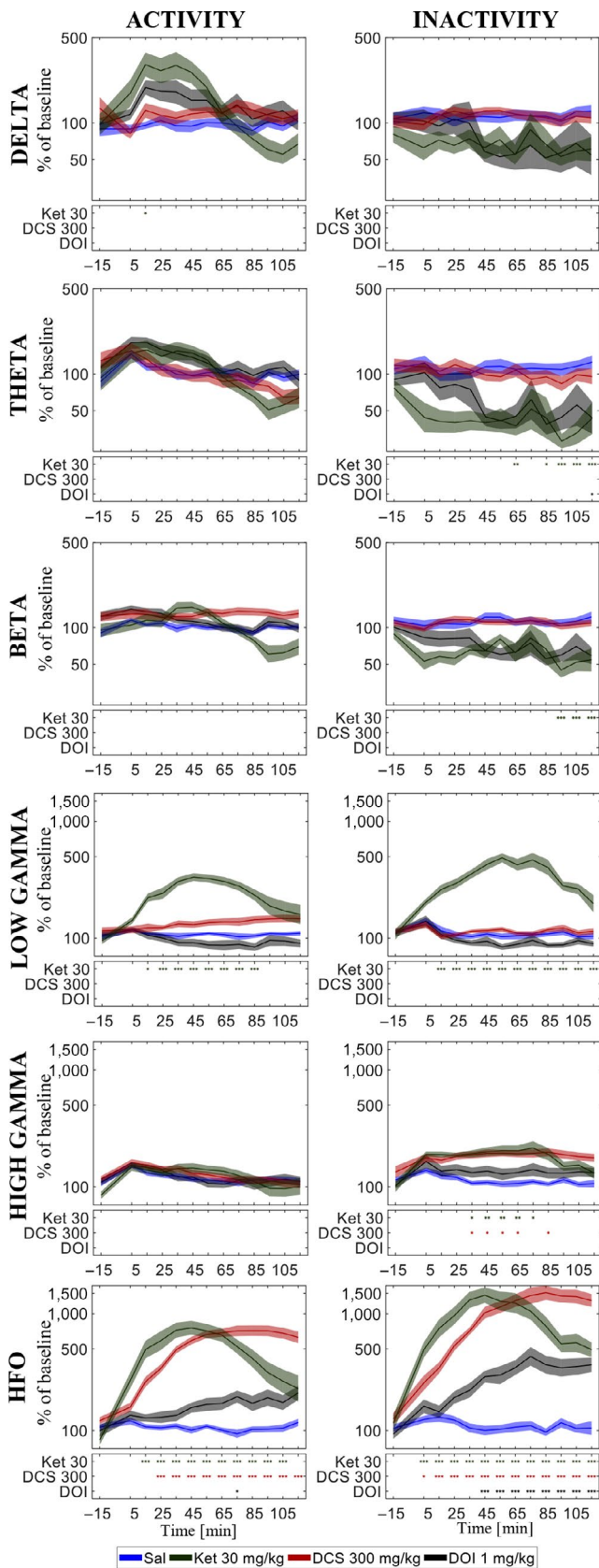


FIGURE 4 Effects of the highest doses of ketamine (Ket), d-cycloserine (DCS) and DOI in the delta, theta, beta, low gamma, high gamma, and HFO frequency bands across the two hours of recording after injection in right medial prefrontal cortex on average over rats. Standard error of the mean (SEM) given as the shaded areas above and below the graphs. Significant differences to saline are shown in the boxes below the graphs when $p < 0.05$ (*), 0.01 (**), or 0.001 (***) [Colour figure can be viewed at wileyonlinelibrary.com]

Low gamma activity

Ketamine induced a peak in the power spectrum in the low gamma range (example in left column of Figure 3b), and the average low gamma increase from baseline was found significantly different to vehicle in all channels and in both locomotive states for the high dose of 30 mg/kg ketamine. For the 10 mg/kg ketamine low gamma activity was significantly enhanced in the ECoG in both states and in the right mPFC in the inactive state. None of the low gamma increases were found to differ significantly between the locomotive states.

High gamma activity

High gamma activity was significantly enhanced by 30 mg/kg ketamine and 300 mg/kg d-cycloserine as compared to vehicle in all channels as well as by 10 mg/kg ketamine in the ECoG in the inactive state. In the active state, only 30 mg/kg ketamine produced a significant increase in the ECoG. The discovered high gamma power increases were for all channels significantly larger in the inactive state as compared to the active state, except at thalamus after 30 mg/kg ketamine dosage (Table 4).

HFO activity

HFO were enhanced significantly both during inactivity and during locomotion in all recorded regions for the 10 and 30 mg/kg doses as well as for the 3 mg/kg dose in left mPFC and in the ECoG. The largest power increases in the HFO band were elicited in the inactive state by 30 mg/kg ketamine in left and right mPFC for which the increase relative to baseline reached 1250 and 1350 percentage points more than vehicle, respectively. The corresponding estimates for the active state were 840 and 673, respectively. The larger HFO enhancement in inactive state as compared to the active state was statistically significant ($P < 0.001$) for all ketamine doses at all recorded areas except for in right mPFC after 3 mg/kg ketamine.

3.4.2 | D-cycloserine

No significant changes in delta, theta, beta, and low gamma activity were found after administration of d-cycloserine.

High gamma activity

In all recording regions, the 300 mg/kg dose of d-cycloserine enhanced high gamma activity in the inactive state only. All

mPFC (one time bin), thalamus, and the ECoG, however, less consistently than in the inactive-state specific analyses.

TABLE 5 Power changes induced by drugs in the total data. [Colour figure can be viewed at wileyonlinelibrary.com]

(a) Left mPFC						
Drug\Freq	δ	θ	β	γ L	γ H	HFO
Ket 30	200			279	88	1151
Ket 10				80		484
Ket 3						112
DCS 300						825
DCS 100						181
Dia						
Amp	142	117	61		84	
DOI						228
(b) Right mPFC						
Drug\Freq	δ	θ	β	γ L	γ H	HFO
Ket 30	176	71	58	304		1036
Ket 10				95		607
Ket 3					53	
DCS 300						1160
DCS 100						134
Dia						
Amp						
DOI						213
(c) Thalamus						
Drug\Freq	δ	θ	β	γ L	γ H	HFO
Ket 30	263		45	144	123	724
Ket 10			41			366
Ket 3			35			
DCS 300		51				724
DCS 100						
Dia						
Amp		105	58			
DOI			48			207
(d) ECoG						
Drug\Freq	δ	θ	β	γ L	γ H	HFO
Ket 30		36	41	395	135	728
Ket 10		47	47	163	72	305
Ket 3						92
DCS 300						579
DCS 100						107
Dia			52			
Amp		77			60	
DOI	65	49	53			193

Note. Tables mark pharmacologically induced changes to a frequency band as recorded in the total data which was found significantly different than vehicle in one or more time-bins within the 2 hr of recording after injection (12 time bins). Significant increases are marked with red and significant decreases are marked with blue. The numbers within colour-coded cells show the difference between compound and vehicle induced changes from baseline (in percentage points), and only the largest difference found over the 12 time bins is given. The estimated differences between a compound and vehicle are determined based on the log-transformed estimates of the fitted statistical model.

changes in the inactive state were significantly larger than in the active state, and in the total data the high gamma increase was not significant. The 100 mg/kg dose of d-cycloserine elicited no significant effect compared to vehicle.

HFO activity

Both doses of d-cycloserine enhanced HFO significantly at all recording areas except for in thalamus after the low 100 mg/kg dosage. The HFO enhancements induced by the high dose were significantly larger in the inactive state compared with the active state and the same was found for the low dose in left mPFC (Tables 3 and 4). In the inactive state, the large dose of d-cycloserine consistently produced significant increase right after injection till the end of recording (120 min after) while in the active state significant differences from vehicle were found from 20 to 30 min after injection (example shown in Figure 4).

3.4.3 | Doi

Delta activity

DOI suppressed delta activity exclusively in the inactive state in thalamus and the ECoG (Table 4) with significances found in the interval from 30 to 120 min after administration. The DOI induced suppression was significantly lower than in the active state, where there was a tendency to increase in all LFP channels and a tendency to decrease in the ECoG. Evaluating the effect of DOI on the total data, a suppression was only found in the ECoG.

Theta activity

DOI suppressed power in the theta range exclusively in the inactive state (Tables 3 and 4) with significant effects found in thalamus, the ECoG, and right mPFC starting at 30, 40, and 110 min after injection and present still at the end of recording (after 120 min). In the active state, there was a tendency for DOI to increase theta power in the LFP channels initially after injection, while in the total data power changes appeared biphasic with late power decreases significant at thalamus and the ECoG. Visual inspection of the baseline-corrected power spectra revealed consistent peaks in the high theta range in left mPFC and the ECoG apparent in the total and active state data, also observable in the inactive state data as a small peak riding on a larger broadband decrease across the lower frequencies.

Beta activity

DOI suppressed power in the beta range exclusively in the inactive state (Tables 3 and 4) with significant effects found in thalamus and the ECoG starting at 20 and 30 min after injection, respectively, and still present at the end of recording (after 120 min).

Gamma activity

DOI did not affect low or high gamma activity significantly. At all recording regions and in both active and inactive states

as well as in the total data, there were tendencies towards decreased power in the low gamma band. In the high gamma band, suppression tendencies were only observed in the inactive state.

HFO activity

DOI enhanced HFO in mPFC during locomotion and in all recordings areas during inactivity where the effects were significantly larger than during locomotion (Tables 3 and 4). The induced HFO enhancements were persistent over time starting from 10 to 40 min after injection being still present at the end of recording (example in Figure 4).

3.4.4 | D-amphetamine

Amphetamine produced no significant changes in the inactive state and only a theta-power increase in the active state (Tables 3 and 4). It should be noted that only little data were recorded in the inactive state after amphetamine administration (Figure 3a). In the total data, amphetamine tended to increase power in all frequency bands and at all recording areas. Increases were significant in left mPFC within delta, theta, beta and high gamma bands, in thalamus within theta and beta bands, and in the ECoG within theta and high gamma bands (Table 5). Baseline-corrected power spectra displayed visually distinct peaks in the high theta range in left mPFC and the ECoG apparent in both the active state and the total data.

3.4.5 | Diazepam

Diazepam induced a beta power increase detected in the inactive state and the total data in the ECoG.

4 | DISCUSSION

This study demonstrates the advantage in accounting for the locomotive state when investigating pharmacological modulation of oscillatory activity in rat ECoG/LFP studies. Spectral powers in all examined frequency bands were found altered during rat locomotion, and some of the investigated drugs produced different effects during the inactive state compared with the active state. We developed a precise fully automatic method for detecting periods with and without locomotion on a 1-s basis for which more than 90% of the detected time in both states was correctly classified. Analyzing data selectively from the inactive state allowed for assessing drug effects in the awake state under minimal influence of locomotive behaviours which revealed i.a. locomotion-independent ketamine effects in the theta, beta, low gamma, high gamma, and particularly the HFO band. Analysing data selectively from the active state, on the other hand, revealed effects in the delta-band particularly associated with locomotion. More

TABLE 6 Systems for behavior recognition reporting classification performance

Publication/System	Species	Behaviours	Classifier	Accuracy	Recall	Precision
Crispim-Junior et al. (2017)	Rat	4 locomotion, immobility, rearing, grooming	Multilayer Perceptron Networks	AUC of ROC: 83.6%–97.6%		
van den Boom et al. (2017)	Mouse	1 self-grooming	Additive logistic regression		83.3%	
Farah et al. (2016)	Rat Mouse	3 exploring, rearing, static	SVM (multiple)	Success rate: 87%	Mean recognition rate: 57%–100%	
Belic et al. (2015)	Rat	2 awake resting, actively behaving	SVM	87%–91%	85%–93%	
Wang et al. (2015)	Rat	5	SVM	89%		
Chanchanachitkul et al. (2013)	Rat	2 walking, other behaviour	Neural Networks	73%		
van Dam et al., 2013;	Rat	11	Quadratic classifier	65%–80%	0–86%	
Kabra et al. (2013)	Mouse	2 follow (social), walking	Additive logistic regression	95.6%		
CleverSys (Jhuang et al., 2010)	Mouse	8	-	60.9%	64%	
Burgos-Artizzu, X. P., Dollar, P., Lin, D., Anderson, D. J., & Perona, P. (2012)	Mouse	13	Decision trees		Average recognition rate: 66%	
Zarringhalam et al. (2012)	Mouse	8	HMM	76%	45%–95%	55%–100%
Jhuang et al. (2010)	Mouse	8	HMM SVM	77.3%	76.4%	
HomeCageScan (Steele et al., 2007)	Mouse	17	—			50%–100%
Dollar et al. (2005)	Mouse	5	One nearest neighbour	72%	32%–89%	
Our classification based on Noldus tracking	Rat	2 active, inactive	Logistic regression	70.9%	74%–76%	91%–100%

and generally larger drug-effects were found in the inactive state compared to the active state.

4.1 | Automatic locomotive state detection with high precision

The locomotive-state detection algorithm was designed to classify states with high precision by assigning timepoints to a state only when the probability for the state (as determined by the logistic regression) was high. This procedure left 21% of data unassigned to a locomotive state and sensitivities low (74%–76%), however, of the periods detected in the active and inactive states 91% and 100% were correctly classified. This method favouring precision ensured that subsequent state-specific analyses of LFPs/ECoGs were reliable. Precision is rarely reported (see Table 6) in other publications on methods for classifying rodent behaviour (Belic et al., 2015; Chanchanachitkul, Nanthiyanuragsa, & Rodamporn, 2013; Crispim-Junior, de Azevedo, &

Marino-Neto, 2017; Dollar et al., 2005; Farah et al., 2016; Jhuang et al., 2010; Kabra, Robie, Rivera-Alba, Branson, & Branson, 2013; Steele et al., 2007; van Dam et al., 2013; van den Boom, Pavlidi, Wolf, Mooij, & Willuhn, 2017; Wang, Mirbozorgi, & Ghovanloo, 2015). Previously reported precisions for the detection of rearing, resting, and walking behaviours have been 58%, 70%, and 70%, respectively, for the method proposed by Zarringhalam et al. (2012) as found in mice, and 71%, 96%, and 95%, respectively, for a beta version of HomeCageScan tested by Steele et al. (2007) as found in one mouse only. These methods, however, detected more behaviours (eight and 17) than in the current study which reduce the chance agreement between actual and predicted classes. Later relevant studies in rats have not explicitly reported precision, and their *chance* accuracy is higher than ours, as we intentionally leave some data unassigned. Video-based systems have achieved accuracies of 65%–80% for classification of 11 behaviours (van Dam et al., 2013) and 87% (“success rate”) for classification

of “exploring,” “rearing”, and “static” states (Farah et al., 2016). An accuracy of 89% has been obtained for kinect-based classification of five behaviours in dark conditions (Wang et al., 2015), and 87%–91% for classification of active and resting behaviours based on LFP (Belic et al., 2015). For comparison, the accuracy of human-to-human scoring of mouse behaviour was previously found to be 72% (Jhuang et al., 2010). The automatic method developed for this study was further validated by comparing power spectra of the automatically segmented data to the corresponding power spectra obtained from the manual scoring. With minor exceptions, power in all investigated frequency bands did not differ between the two methods, and both methods yielded the same overall conclusions on how oscillatory activity is affected during locomotion. As the automatic method left less determinable data unclassified (~21% of data), it could be expected to detect more “profound” locomotion than the manual method, which could potentially explain the slight differences observed between the two state detection methods on delta and high gamma power. Similarly, the automatically determined inactive state could contain a larger percentage of motionless-alertness, known to elicit theta waves (Shin, Kim, Bianchi, Wong, & Shin, 2005), which could potentially explain the larger theta power relative to the manually detected inactive state.

The classification method could potentially be improved with high-precision detection of more states using more reliable tracking methods based on, for example, accelerometers or optimized video-tracking. Detecting more states like grooming, rearing, and sleep could yield more detailed knowledge about compound effects. Standard sleep-wake scoring requires recording of the electromyogram (Bastianini et al., 2017), which was not applied in this study. The inactive state detected in this study may contain short periods of sleep although recordings were conducted in the dark period when rats are least likely to sleep.

4.2 | Oscillatory activity altered during spontaneous locomotion in all frequency bands

We found locomotion generally associated with increased powers compared to powers in the inactive state, with the exception that delta and beta oscillations were suppressed in the ECoG. The largest changes were found in the theta, delta, and high gamma bands, pronounced changes were found in the low gamma and HFO bands, while only small or no changes were found in the beta band. The profound, differential, and widespread effect of locomotion across frequency bands and brain areas underline the need to account for locomotive states when analysing oscillatory brain activity in the awake state, particularly when investigating pharmacological drugs that are expected to modulate locomotor activity as for the NMDAR antagonists. It has long been recognized that theta power in the hippocampus is enhanced

during locomotion (Coenen, 1975; Vanderwolf, 1969), whereas changes in other frequency bands in relation to locomotion only have been investigated in few studies: Besides enhanced theta power during locomotion (Harris Bozer et al., 2016; Noga et al., 2017), studying the ventral tegmental area and mesencephalic locomotor region during cocaine-induced and treadmill-forced locomotion, respectively, found power increases in the delta, beta, low gamma, and high gamma bands. These findings are largely in line with our LFP findings for spontaneous locomotion in drug-free rats. Potential differences between brain regions and additional effects introduced from the artificial induction of locomotion in other studies should however be borne in mind.

4.3 | Pharmacological modulation of locomotion

Using the automatic state-detector for investigating changes in locomotor activity induced by ketamine (3, 10, and 30 mg/kg), d-cycloserine (100 and 300 mg/kg), DOI (1 mg/kg), d-amphetamine (1 mg/kg), and diazepam (1 mg/kg), we found altered time spent in each state after d-amphetamine and ketamine administration (Figure 3a). The distinct increase in locomotor activity induced by 1 mg/kg amphetamine was expected (Broersen, Feldon, & Weiner, 1999; Fink & Smith, 1979; Hunt et al., 2006) but 1 mg/kg diazepam did not significantly decrease the time spent in the active state. Diazepam has previously been shown to induce mild sedation at doses down to 0.2 mg/kg (Coenen & van Luijtelaaar, 1989; Elliot & White, 2001; Schmitt & Hiemke, 1998). The lack of significant locomotor effects in this study by 1 mg/kg of diazepam could potentially be too low given our study design. As the rats in the present study were fully habituated a significant further reduction in the activity level may have been impeded. Studies with less habituated rats and higher doses of sedating compounds may show the sensitivity for reduction of locomotor activity. However, the automatic state-detector did register a reduction in time spent in the active state by 3 mg/kg of ketamine. The dose of 10 mg/kg ketamine induced no detectable change, whereas 30 mg/kg doses of ketamine increased the amount of time spent in the active state. The detected time spent in active and inactive states could deviate slightly from the true time spent in the two states as the developed state-detection algorithm rejected ~23% of data as “behaviourally indistinct,” however, the detected changes in video scored locomotor activity were similar to those assessed with infrared beam breaks. Our findings align with previous investigations in rats showing increases in locomotor activity at ketamine doses of ≥ 12 mg/kg (Caixeta et al., 2013; Hunt et al., 2006; Imre et al., 2006; Matulewicz et al., 2010; Nicolás et al., 2011; Páleníček et al., 2011), decreases (Cordon et al., 2015; Kealy et al., 2017; Kocsis, 2012; Nicolás et al., 2011) or no change (Engin, Treit, & Dickson, 2009; Gigliucci et al., 2013) at 10 mg/kg, and mainly no effect at doses between 0.25 and 5 mg/kg (Akinfiresoye & Tizabi,

2013; Imre et al., 2006; Réus et al., 2011; Tizabi, Bhatti, Manaye, Das, & Akinfiresoye, 2012).

4.4 | Locomotive-state specific analyses of field potentials: Overcoming hyperlocomotion-induced effects and discovering state-dependency of pharmacological modulations

The significant alterations in oscillatory activity during locomotion show that electrophysiological effects of a pharmacological compound may be largely influenced by induced changes in the total duration of active locomotion, which can cause false interpretation of the impact of the compound on the brain. To overcome this pitfall in the evaluation of pharmacological modulation of brain signalling, locomotion has previously been controlled by placing rodents on a rotating drum (Krijzer et al., 1993; Visser et al., 2003), animals have been sedated or anaesthetized (Hakami et al., 2009), or behaviours have been scored manually (Coenen & van Luijckelaar, 1989; van Lier et al., 2004) or with computational methods (Lee et al., 2017; Niell & Stryker, 2010) in order to investigate the pharmacological modulation for one type of behaviour specifically. Some drawbacks of these methods are that (a) forced locomotion can be expected to impose more noise, motion-related artefacts, and brain signalling related to locomotion in the signals, and for low speeds a constant level of locomotor activity may not be ensured, (b) sedated or anesthetized brain states may not reflect the awake state, (c) manual scoring of spontaneous behaviour is strenuous and tedious work with low time-resolution, and (d) lack of validation of computational methods for behaviour scoring prevents assessment of the credibility of results. Recently (Lee et al., 2017), investigated behaviour-specific effects of NMDAR-antagonists using a measure of “distance travelled” obtained with EthoVision to classify stationary, walking and running behaviours in long epochs of 5 min. Lee et al. (2017) did not report how consistently a behaviour is expressed within the 5 min and therefore their results showing no state-dependency of gamma and HFO cannot be compared directly to ours. The automatic method developed in this study detected periods of rat locomotion and inactivity on a second-by-second basis with high precision allowing us to analyse recorded field potentials specifically for each behavioural state in an objective manner and with high certainty that the detected periods of active and inactive behaviours were assigned to the correct class of behaviour. The recorded field potentials were segmented according to locomotive state both during baseline and after drug administration enabling evaluation of drug-effects specifically within one state where the baseline data used as reference was acquired within the same state. No change would be expected in this state-specific baseline-corrected measure if the compound simply altered the percentage of time spent in the locomotive state, and the

differences in oscillatory activity expressed in the two states should not affect the estimation of change relative to baseline. Our locomotive state-specific analyses thus allow for (a) obtaining measurements of drug-effects on LFP/ECOG affected only little by changes in the occurrence of locomotion, (b) indicating whether drug effects are associated with a particular behavioural state, and (c) clarifying whether previously observed effects of drugs in non-segmented data could be related to changes in time spent in locomotion.

Drug-effects observed specifically in the inactive state should reflect changes in neuronal functioning and not simply changes in locomotor states. Such locomotion independent drug-effects were found in the theta, beta, low gamma, high gamma and HFO bands induced by ketamine, d-cycloserine and DOI. Overall, more and generally larger effects were found in the inactive state as compared with the active state. Drug-induced changes could be expressed in one state only due to either (a) specific expression within the state or (b) simply due to larger variance in the other state producing a statistically insignificant result. However, in the lower frequency bands, we found effects in one state not present even as a tendency in the other state. Our study thus exemplifies how, quantifying spectral power changes within each locomotive state specifically, can provide more precise and detailed estimates of how drugs affect brain signalling and allows for discovering state-dependent effect as shown through administration of ketamine, d-cycloserine, DOI, amphetamine, and diazepam described further below.

4.4.1 | Pharmacological findings

Delta, theta

In our study, ketamine at the highest dose tested (30 mg/kg) induced an overall increase in delta power that was solely driven by the data recorded during the active state. NMDAR-antagonists including ketamine have been found to produce both increases and decreases in delta activity (see review by Hunt & Kasicki, 2013), and directly inconsistent results have been found over frontal cortex for the same dose (0.1 mg/kg) of MK-801 (Dimpfel & Spüler, 1990; Ehlers, Kaneko, Wall, & Chaplin, 1992). Given our results, conflicting findings could arise if the percentages of data recorded during locomotion have varied across studies. The ketamine-induced change in delta activity from baseline to post-injection locomotion could reflect changes in the characteristics of the expressed locomotor activity such as locomotion speed known to correlate with delta power (Nicolás et al., 2011) or motor incoordination induced by ketamine (Zanos et al., 2016). The increased locomotion by amphetamine could also partly explain an increase in delta power in one of the four recording sites (left mPFC) in our study. DOI on the other hand inhibited delta, theta and beta power and most pronounced during the inactive state. A broadband decrease of power is in line with previous reports of serotonergic hallucinogens (predominantly acting

through 5-HT_{2A} agonism) producing decreased power in a broad range of lower frequencies up to 20 Hz across cortical (Riba et al., 2002) and subcortical regions (Kometer, Pokorny, Seifritz, & Volleinweider, 2015) in humans. In freely moving rats, DOI has produced suppressions across the delta, theta, and beta bands in frontal cortex (Dimpfel & Spüler, 1990; Hiyoshi, Kambe, Karasawa, & Chaki, 2014b) in line with our results, though power increases have been reported in the 7.00–9.50 Hz range (Dimpfel & Spüler, 1990) not evaluated separately in this study. Ketamine also depressed theta and beta power but in the inactive state only, which to a lesser degree was also recapitulated in the total data. Previous studies of NMDAR antagonists have found both increases and decreases in theta activity in the areas investigated in this study (Buzsáki, 1991; Dimpfel & Spüler, 1990; Ehlers et al., 1992; Kittelberger, Hur, Sazegar, Keshavan, & Kocsis, 2012; Páleníček et al., 2011; Sebban, Tesolin-Decros, Ciprian-Ollivier, Perret, & Spedding, 2002). Factors affecting the extent of locomotion expressed during recordings used in previous analyses, such as animal strain (van Lier, Drinkenburg, & Coenen, 2003), habituation time, or extensiveness of artefact rejection, could at least partially explain the very diverse previous findings on NMDAR antagonist effects on delta and theta oscillations profoundly affected by locomotion.

Beta

In the mPFC, beta activity has been found suppressed for lower doses of PCP while larger doses (expected to induce more locomotion) have produced overall elevation of the power spectra (Páleníček et al., 2011; Sebban et al., 2002). NMDAR antagonists have been found to decrease low beta activity (Dimpfel & Spüler, 1990) and increase high beta activity (Kulikova et al., 2012; Páleníček et al., 2011). In our study, ketamine and DOI produced beta activity suppression occurring specifically in the inactive state and the suppression was also observable in the total data. Ketamine-induced suppression of beta power appears stable across species as decreases have also been found in LFPs from mice (Lazarewicz et al., 2010), vervet monkeys (Slovik et al., 2017) and in human EEG (Knott et al., 2006) and MEG recordings (Muthukumaraswamy et al., 2015; Rivolta et al., 2015). Only one human study did not find any effect of ketamine on current densities in the beta band (de La Salle et al., 2016). Thus, ketamine-effects in sedentary humans resemble suppressions in rats emerging specifically during inactivity. Diazepam enhanced beta power as consistently found in rats (Coenen & van Luijckelaar, 1989; van Lier et al., 2004; Visser et al., 2003), mice (Scheffzük et al., 2013), and cats (Hashimoto, Hamada, Wada, & Fukuda, 1992).

Gamma

Across the drugs investigated in this study, only ketamine elicited changes in the low gamma band, while both ketamine

and d-cycloserine enhanced high gamma activity. The low gamma enhancement occurred irrespective of state, while high gamma activity was enhanced almost exclusively in the inactive state.

Non-competitive NMDAR antagonists are well-known to induce widespread gamma activity in resting state shown in humans (Nugent et al., 2018; Rivolta et al., 2015; Schultz, Schultz, Zachen, & Pichlmayr, 1990; Schwartz, Virden, & Scott, 1974) and in freely moving rats (Hiyoshi, Hikichi, Karasawa, & Chaki, 2014a; Hunt & Kasicki, 2013; Kealy et al., 2017; Lee et al., 2017) also shown specifically in thalamus (Zhang, Yoshida, Katz, & Lisman, 2012), and for both low and high gamma bands in frontal cortex (Kittelberger et al., 2012; Kocsis, 2012) and PFC (Lee et al., 2017; Wood, Kim, & Moghaddam, 2012). In frontal cortex, low gamma activity was previously found increased by NMDAR antagonists selective to NR2A subunit containing receptors, while high gamma activity was increased by both NR2A and NR2B selective antagonists, although some findings were inconsistent (Kocsis, 2012). That d-cycloserine selectively increased high but not low gamma could potentially reflect the limited modulation of d-cycloserine at NR1/NR2A receptors and the reduced efficacy (65% of glycine) at NR1/NR2B receptors (Dravid et al., 2010). Ketamine, on the other hand, being a non-selective antagonist, could be expected to elicit both low and high gamma as observed.

Gamma rhythms have been found mediated by interneurons (Buzsáki & Wang, 2012) with peak-frequency depending on NMDAR activity at least in entorhinal cortex (Middleton et al., 2008). Ketamine and MK-801 induced gamma activity has previously been found positively correlated with the induced hyperlocomotion (Hakami et al., 2009; Molina, Skelin, & Gruber, 2014) with higher correlations to locomotion speed found for high gamma power than low (Nicolás et al., 2011), which is supported by our findings of increased gamma activity in drug-free locomotion particularly in the higher gamma band. Our findings that high gamma effects of ketamine and d-cycloserine are locomotor activity dependent, and that the effect of d-cycloserine was not significant when evaluated on total data, show the potential of state-specific analysis to reduce inconsistent results in the field.

Hfo

Substantial HFO increases were recorded after administration of ketamine and d-cycloserine as well as DOI. HFO power was increased in the total and active state data, but approximately twofold more in the inactive state. The differences between the two states, could only partly be explained by higher baseline-levels of HFO power in the active state, as HFO power was only found increased by 112%–118% during locomotion as compared to during inactivity based on the automatic state-detection. The profound and widespread enhancements of HFO elicited by ketamine, d-cycloserine

and DOI in this study, are in line with previous findings of large power increases in HFO produced by non-competitive NMDAR antagonists found *i.a.* over frontal cortex (Hiyoshi et al., 2014b), in PFC (Lee et al., 2017; Olszewski, Dolowa, Matulewicz, Kasicki, & Hunt, 2013), and in posterior thalamus (Hunt, Falinska, Łeski, Wójcik, & Kasicki, 2011). Despite previous findings of association between locomotor activity and power of NMDAR-antagonist induced HFO (Hunt et al., 2006; Lee et al., 2017; Nicolás et al., 2011), also supported by our findings of increased HFO power during drug-free locomotion, we find that HFO is elicited independently of locomotion in line with the suggestion in the very first publication on HFO (Hunt et al., 2006) in rats. Here, Hunt et al. motivated that no functional relationship between NMDAR-antagonist induced HFO and locomotor activity necessarily exists despite the correlational relationship, a point subsequently supported by (Pinault, 2008) and (Matulewicz et al., 2010). In this study, it is striking that ketamine and d-cycloserine express similar effects on network activity only on HFO and high gamma. It will be of great interest to investigate how subunit-selective NMDAR modulators affect HFO.

Besides different modes of action at the NMDAR receptor, effects of ketamine and d-cycloserine could differ due to ketamine affecting a broad variety other receptors and neurotransmitter systems including the dopaminergic, noradrenergic, and serotonergic systems (Hara et al., 1998; Kapur & Seeman, 2002; Pham et al., 2017; Yamamoto et al., 2013). Specifically, in mPFC, ketamine has been found to increase the extracellular levels of 5-HT within the first 2 hr after ketamine administration (Pham et al., 2017). Understanding the basis of the inactivity-dependent suppressions in the lower frequencies is not straight forward. In humans administered ketamine, ratings of depersonalization have been associated with suppressed alpha (8–12.5 Hz) activity in particular (de La Salle et al., 2016), and state-dependent psychotomimetic has been found by (Powers, Gancsos, Finn, Morgan, & Corlett, 2015) who observed psychosis resemblances (auditory verbal hallucinations) specifically within a reduced perceptual environment. Whether the observed inactivity dependent broad suppressions across the theta and (in particular lower) beta bands induced by both ketamine and DOI are directly associated with 5-HT mediated psychotomimetic effects remains to be investigated and requires measures taken to account for locomotive states. The mechanisms underlying HFO power increases (constituting the largest effects of our study by far) are also unclear. In humans, extra-ocular and superficial muscles have not been found to induce HFO (Nottage & Horder, 2015) indicating a cerebral origin of the oscillations, and ripple (125–250 Hz) episodes has been found increased during cognitive processing (Kucewicz et al., 2014). In rats, HFO (130–180 Hz) have been associated with behavioural states where generation of mental activity is most intense (Hunt

et al., 2009). Intriguingly, HFO enhancements in rats have been found induced not only by NMDAR-antagonists and hallucinogens but also by antipsychotics (Goda et al., 2013; Hunt, Olszewski, Piasecka, Whittington, & Kasicki, 2015) indicating that further clarification of the mechanisms affecting HFO and proper control for influential factors is needed. With our study, future research clarifying mechanisms underlying HFO, can now proceed knowing that locomotor activity is not a primary driver of HFO induced by NMDAR and 5-HT_{2A} modulators.

4.5 | Perspectives for drug development

As stated by (Denayer et al., 2017): Even the best validated animal model cannot yield conclusive data when the experimental design is flawed or study-execution not well controlled. Given the pronounced alterations in ECoG and LFP recordings during locomotion, it is imperative to account for locomotion in preclinical pharmac-EEG studies to know if drug-induced changes in LFP/ECoG are simply reflecting induced hypo-/hyperlocomotion, or if any locomotion-independent drug-effects are concealed or exaggerated by locomotion-related changes in oscillatory activity. In resting state pharmac-EEG studies in humans, the behavioural and awareness states of the subjects are well-controlled and subjects are in a (semi-) reclined comfortable position (Jobert et al., 2012). Locomotion is thus not occurring in pharmac-EEG studies in humans, underpinning the importance of removing data recorded during rat locomotion in preclinical research/animal studies intended for translation. In human resting state conditions, head-fixation is, furthermore, not recommended as it constitutes a task (Jobert et al., 2012). This indicates that preclinical studies employing state-detection in freely moving (non-sedated) animals provide better opportunities for translation compared to, for example, monitoring the rotation of a spherical treadmill under a head-fixed rodent. Manual detection of the behavioural states is tedious, time-consuming, and has low time resolution for which reason automatic classification of behaviour is highly desirable and in many cases the only realistic option, however, confidence in state-specific analyses of drug-induced LFP/ECoG changes depend entirely on the precision of the automatic classification. Viable and validated methods for behaviour recognition has previously been proposed, however, precisions are in most cases not reported, and studies investigating LFP/ECoG recordings specifically for particular automatically detected behaviours use methods which are not validated. We show in this study, that it is possible to classify two states with and without locomotion in very short epochs with high precision. The high classification precision provides the possibility for detecting differences between the states, and enables the discovery of drug-effects associated exclusively with one state which can be concealed if effects are evaluated based on the total data, as exemplified in our

study. State-specific analyses of amphetamine, on the other hand, showed that the effects seen on total data was largely driven by the induced hyperlocomotion.

Evaluating drug-effects specifically during inactive state has the advantage that estimated drug-effects should not reflect any locomotion-related matter, and the recording conditions are more similar to those of clinical studies. Generally, in scientific experimentation, it is important to remove or at least (statistically) account for nuisance factors influencing measurements in order to obtain accurate estimates of the effects under investigation, nevertheless, at present the majority of animal studies investigating electrophysiological effects of pharmacological compounds do not provide any type of behaviour-specific evaluations, which may impede discoveries in the field. Differences in the amount of locomotion during recording, for example, arising from differences in rat strain, habituation period and extent of artefact rejection, could potentially account for many of the conflicting findings made previously particularly in delta and theta activity alterations induced by NMDAR antagonists (see review by Hunt & Kasicki, 2013). Hopefully, inconsistencies between rodent experiments will decrease further with behaviour-specific analyses and yield more detailed and accurate estimation of drug-effects. However, excluding data recorded during locomotion can already now make recording conditions for pharmacology-EEG studies in animals more similar to human EEG and thereby improve prediction of drug-efficacy in the clinic.

ACKNOWLEDGEMENT

The authors thank Kasper Larsen for data collection and the results attached in Supporting Information Figure S1, Christian Spang Pedersen for results in Supporting Information Figure S2, as well as Dat Chau Le for providing knowledge on issues with Noldus tracking.

CONFLICT OF INTEREST

The authors state no conflict of interest.

DATA ACCESSIBILITY

Data not available.

AUTHORS' CONTRIBUTIONS

Hansen, I. H.: Drafted paper, analysed data, developed locomotive state detection method. Agerskov, C.: Analysed data, drafted two data analysis sections. Arvastson, L.: Supervised data analyses and edited manuscript. Sorensen, H. B. D.: Supervised data analyses and edited manuscript. Bastlund, J. F.: Contributed to the conception of the work

and interpretation of data and edited manuscript. Herrik, K. F.: Designed study and drafted paper.

ORCID

Ingeborg H. Hansen  <https://orcid.org/0000-0002-2881-6875>

Claus Agerskov  <https://orcid.org/0000-0003-2244-713X>

REFERENCES

- Ahnaou, A., Huysmans, H., Biermans, R., Manyakov, N. V., & Drinkenburg, W. H. I. M. (2017). Ketamine: Differential neurophysiological dynamics in functional networks in the rat brain. *Translational Psychiatry*, 7, e1237. <https://doi.org/10.1038/tp.2017.198>
- Ahnaou, A., Huysmans, H., van de Castele, T., & Drinkenburg, W. H. I. M. (2017). Cortical high gamma network oscillations and connectivity: A translational index for antipsychotics to normalize aberrant neurophysiological activity. *Translational Psychiatry*, 7, 1285.
- Akinfiresoye, L., & Tizabi, Y. (2013). Antidepressant effects of AMPA and ketamine combination: Role of hippocampal BDNF, synapsin, and mTOR. *Psychopharmacology (Berl)*, 230, 291–298. <https://doi.org/10.1007/s00213-013-3153-2>
- Amat-Foraster, M., Jensen, A. A., Plath, N., Herrik, K. F., Celada, P., & Artigas, F. (2018). Temporally dissociable effects of ketamine on neuronal discharge and gamma oscillations in rat thalamocortical networks. *Neuropharmacology*, 137, 13–23. <https://doi.org/10.1016/j.neuropharm.2018.04.022>
- Ayaz, A., Saleem, A. B., Schölvinck, M. L., & Carandini, M. (2013). Locomotion controls spatial integration in mouse visual cortex. *Current Biology*, 23, 890–894. <https://doi.org/10.1016/j.cub.2013.04.012>
- Bastianini, S., Alvente, S., Berteotti, C., Lo Martire, V., Silvani, A., Swoap, S. J., ... Cohen, G. (2017). Accurate discrimination of the wake-sleep states of mice using non-invasive whole-body plethysmography. *Scientific Reports*, 7, 41698. <https://doi.org/10.1038/srep41698>
- Belic, J., Halje, P., Richter, U., Petersson, P., & Kotaleski, J. H. (2015). Behavior discrimination using a discrete wavelet based approach for feature extraction on local field potentials in the cortex and striatum. *Proceedings of the 7th Annual International IEEE EMBS Conference on Neural Engineering*. Montpellier.
- Broersen, L. M., Feldon, J., & Weiner, I. (1999). Dissociative effects of apomorphine infusions into the medial prefrontal cortex of rats on latent inhibition, prepulse inhibition and amphetamine-induced locomotion. *Neuroscience*, 94, 39–46.
- Burgos-Artizzu, X. P., Dollar, P., Lin, D., Anderson, D. J., & Perona, P. (2012). Social behavior recognition in continuous video. *Proceedings of the IEEE Computer Society Conference on Computer Vision and Pattern Recognition*. IEEE.
- Buzsáki, G. (1991). The thalamic clock: Emergent network properties. *Neuroscience*, 41, 351–364.
- Buzsáki, G., & Wang, X.-J. (2012). Mechanisms of gamma oscillations. *Annual Review of Neuroscience*, 35, 203–225. <https://doi.org/10.1146/annurev-neuro-062111-150444>
- Caixeta, F. V., Cornélio, A. M., Scheffer-Teixeira, R., Ribeiro, S., & Tort, A. B. L. (2013). Ketamine alters oscillatory coupling in the hippocampus. *Scientific Reports*, 3, 2348.

- Chanchanachitkul, W., Nanthiyaturagsa, P., & Rodamporn, S. (2013). 2013 6th Biomedical Engineering International Conference (BMEiCON): 23–25 Oct. 2013, Krabi, Thailand.
- Coenen, A. M. L. (1975). Frequency analysis of rat hippocampal electrical activity. *Physiology & Behavior*, *14*, 391–394.
- Coenen, A. M. L., & van Luijckelaar, E. L. J. M. (1989). Effects of diazepam and two beta-carbolines on epileptic activity and on EEG and behavior in rats with absence seizures. *Pharmacology Biochemistry and Behavior*, *32*, 27–35.
- Cordon, I., Nicolás, M. J., Arrieta, S., Lopetegui, E., López-Azcárate, J., Alegre, M., ... Valencia, M. (2015). Coupling in the cortico-basal ganglia circuit is aberrant in the ketamine model of schizophrenia. *European Neuropsychopharmacology*, *25*, 1375–1387. <https://doi.org/10.1016/j.euroneuro.2015.04.004>
- Crispim-Junior, C. F., de Azevedo, F. M., & Marino-Neto, J. (2017). What is my rat doing? Behavior understanding of laboratory animals. *Pattern Recognition Letters*, *94*, 134–143.
- Denayer, T., Stöhr, T., & van Roy, M. (2017). Animal models in translational medicine: Validation and prediction. *European Journal of Molecular & Clinical Medicine*, *2*, 5.
- de La Salle, S., Choueiry, J., Shah, D., Bowers, H., McIntosh, J., Ilivitsky, V., & Knott, V. (2016). Effects of ketamine on resting-state EEG activity and their relationship to perceptual/dissociative symptoms in healthy humans. *Frontiers in Pharmacology*, *7*, 348. <https://doi.org/10.3389/fphar.2016.00348>
- Dimpfel, W., & Spüler, M. (1990). Dizocilpine (MK-801), ketamine and phencyclidine: Low doses affect brain field potentials in the freely moving rat in the same way as activation of dopaminergic transmission. *Psychopharmacologia*, *101*, 317–323.
- Dollar, P., Rabaud, V., Garrison, C., & Belongie, S. (2005). Behavior recognition via sparse spatio-temporal features. *Proceedings 2nd Joint IEEE International Workshop on Visual Surveillance and Performance Evaluation of Tracking and Surveillance (VS-PETS)*. Beijing.
- Dravid, S. M., Burger, P. B., Prakash, A., Geballe, M. T., Yadav, R., Le, P., ... Traynelis, S. F. (2010). Structural determinants of D-cycloserine efficacy at the NR1/NR2C NMDA receptors. *Journal of Neuroscience*, *30*, 2741–2754. <https://doi.org/10.1523/JNEUROSCI.5390-09.2010>
- Duda, R. O., & Hart, P. E. (1973). *Pattern classification and scene analysis*. New York, NY: Wiley.
- Ehlers, C. L., Kaneko, W. M., Wall, T. L., & Chaplin, R. I. (1992). Effects of dizocilpine (MK-801) and ethanol on the EEG and event-related potentials (ERPs) in rats. *Neuropharmacology*, *31*, 369–378.
- Elliot, E. E., & White, J. M. (2001). The acute effects of zolpidem compared to diazepam and lorazepam using radiotelemetry. *Neuropharmacology*, *40*, 717–721.
- Engin, E., Treit, D., & Dickson, C. T. (2009). Anxiolytic- and antidepressant-like properties of ketamine in behavioral and neurophysiological animal models. *Neuroscience*, *161*, 359–369.
- Farah, R., Langlois, J. M. P., & Bilodeau, G.-A. (2016). Computing a rodent's diary. *Signal, Image and Video Processing*, *10*, 567–574.
- Fink, J. S., & Smith, G. P. (1979). Abnormal pattern of amphetamine locomotion after 6-OHDA lesion of anteromedial caudate. *Pharmacology Biochemistry and Behavior*, *11*, 23–30.
- Furth, K. E., McCoy, A. J., Dodge, C., Walters, J. R., Buonanno, A., & Delaville, C. (2017). Neuronal correlates of ketamine and walking induced gamma oscillations in the medial prefrontal cortex and mediodorsal thalamus. *PLoS ONE*, *12*, e0186732.
- Gigliucci, V., O'Dowd, G., Casey, S., Egan, D., Gibney, S., & Harkin, A. (2013). Ketamine elicits sustained antidepressant-like activity via a serotonin-dependent mechanism. *Psychopharmacology (Berl)*, *228*, 157–166.
- Goda, S. A., Piasecka, J., Olszewski, M., Kasicki, S., & Hunt, M. J. (2013). Serotonergic hallucinogens differentially modify gamma and high frequency oscillations in the rat nucleus accumbens. *Psychopharmacology (Berl)*, *228*, 271–282.
- Goff, D. C. (2017). D-cycloserine in schizophrenia: New strategies for improving clinical outcomes by enhancing plasticity. *Current Neuropharmacology*, *15*, 21–34.
- Hakami, T., Jones, N. C., Tolmacheva, E. A., Gaudias, J., Chaumont, J., Salzberg, M., ... Pinault, D. (2009). NMDA receptor hypofunction leads to generalized and persistent aberrant gamma oscillations independent of hyperlocomotion and the state of consciousness. *PLoS ONE*, *4*, e6755.
- Hara, K., Yanagihara, N., Minami, K., Ueno, S., Toyohira, Y., Sata, T., ... Izumi, F. (1998). Ketamine interacts with the noradrenaline transporter at a site partly overlapping the desipramine binding site. *Naunyn-Schmiedeberg's Archives of Pharmacology*, *358*, 328–333.
- Harris Bozer, A. L., Li, A.-L., Sibi, J. E., Bobzean, S. A. M., Peng, Y. B., & Perrotti, L. I. (2016). Local field potentials in the ventral tegmental area during cocaine-induced locomotor activation: Measurements in freely moving rats. *Brain Research Bulletin*, *121*, 186–191.
- Hashimoto, T., Hamada, C., Wada, T., & Fukuda, N. (1992). Comparative study on the behavioral and EEG changes induced by diazepam, buspirone and a novel anxiolytic, DN-2327, in the cat. *Neuropsychobiology*, *26*, 89–99.
- Hayes, M. H. (1996). *Statistical digital signal processing and modeling*. Hoboken, New Jersey: Wiley.
- Heresco-Levy, U., Gelfin, G., Bloch, B., Levin, R., Edelman, S., Javitt, D. C., & Kremer, I. (2013). A randomized add-on trial of high-dose D-cycloserine for treatment-resistant depression. *International Journal of Neuropsychopharmacology*, *16*, 501–506.
- Hiyoshi, T., Hikichi, H., Karasawa, J.-I., & Chaki, S. (2014a). Metabotropic glutamate receptors regulate cortical gamma hyperactivities elicited by ketamine in rats. *Neuroscience Letters*, *567*, 30–34.
- Hiyoshi, T., Kambe, D., Karasawa, J.-I., & Chaki, S. (2014b). Differential effects of NMDA receptor antagonists at lower and higher doses on basal gamma band oscillation power in rat cortical electroencephalograms. *Neuropharmacology*, *85*, 384–396.
- Hocking, R. R. (1976). A Biometrics Invited Paper. The analysis and selection of variables in linear regression. *Biometrics*, *32*(1), 1–49.
- Hood, W. F., Compton, R. P., & Monahan, J. B. (1989). D-cycloserine: A ligand for the N-methyl-D-aspartate coupled glycine receptor has partial agonist characteristics. *Neuroscience Letters*, *98*, 91–95.
- Hunt, M. J., Falinska, M., Łeski, S., Wójcik, D. K., & Kasicki, S. (2011). Differential effects produced by ketamine on oscillatory activity recorded in the rat hippocampus, dorsal striatum and nucleus accumbens. *Journal of Psychopharmacology*, *25*, 808–821.
- Hunt, M. J., & Kasicki, S. (2013). A systematic review of the effects of NMDA receptor antagonists on oscillatory activity recorded in vivo. *Journal of Psychopharmacology*, *27*, 972–986.
- Hunt, M. J., Matulewicz, P., Gottesmann, C., & Kasicki, S. (2009). State-dependent changes in high-frequency oscillations recorded in the rat nucleus accumbens. *Neuroscience*, *164*, 380–386.

- Hunt, M. J., Olszewski, M., Piasecka, J., Whittington, M. A., & Kasicki, S. (2015). Effects of NMDA receptor antagonists and antipsychotics on high frequency oscillations recorded in the nucleus accumbens of freely moving mice. *Psychopharmacology (Berl)*, *232*, 4525–4535.
- Hunt, M. J., Raynaud, B., & Garcia, R. (2006). Ketamine dose-dependently induces high-frequency oscillations in the nucleus accumbens in freely moving rats. *Biological Psychiatry*, *60*, 1206–1214.
- Imre, G., Fokkema, D. S., Den Boer, J. A., & Ter Horst, G. J. (2006). Dose-response characteristics of ketamine effect on locomotion, cognitive function and central neuronal activity. *Brain Research Bulletin*, *69*, 338–345.
- Jhuang, H., Garrote, E., Mutch, J., Yu, X., Khilnani, V., Poggio, T., ... Serre, T. (2010). Automated home-cage behavioural phenotyping of mice. *Nature Communications*, *1*, 68.
- Jobert, M., Wilson, F. J., Ruigt, G. S. F., Brunovsky, M., Pritchep, L. S., & Drinkenburg, W. H. I. M. (2012). Guidelines for the recording and evaluation of pharmaco-EEG data in man: The International Pharmaco-EEG Society (IPEG). *Neuropsychobiology*, *66*, 201–220.
- Kabra, M., Robie, A. A., Rivera-Alba, M., Branson, S., & Branson, K. (2013). JAABA: Interactive machine learning for automatic annotation of animal behavior. *Nature Methods*, *10*, 64–67.
- Kapur, S., & Seeman, P. (2002). NMDA receptor antagonists ketamine and PCP have direct effects on the dopamine D(2) and serotonin 5-HT(2) receptors-implications for models of schizophrenia. *Molecular Psychiatry*, *7*, 837–844.
- Kealy, J., Commins, S., & Lowry, J. P. (2017). The effect of NMDA-R antagonism on simultaneously acquired local field potentials and tissue oxygen levels in the brains of freely-moving rats. *Neuropharmacology*, *116*, 343–350.
- Keller, G. B., Bonhoeffer, T., & Hübener, M. (2012). Sensorimotor mismatch signals in primary visual cortex of the behaving mouse. *Neuron*, *74*, 809–815.
- Kislin, M., Mugantseva, E., Molotkov, D., Kuleskaya, N., Khirug, S., Kirilkin, I., ... Khiroug, L. (2014). Flat-floored air-lifted platform: A new method for combining behavior with microscopy or electrophysiology on awake freely moving rodents. *Journal of Visualized Experiments: JoVE* (88), e51869. <https://doi.org/10.3791/51869>
- Kittelberger, K., Hur, E. E., Sazegar, S., Keshavan, V., & Kocsis, B. (2012). Comparison of the effects of acute and chronic administration of ketamine on hippocampal oscillations: Relevance for the NMDA receptor hypofunction model of schizophrenia. *Brain Structure and Function*, *217*, 395–409.
- Knott, V., McIntosh, J., Millar, A., Fisher, D., Villeneuve, C., Ilivitsky, V., & Horn, E. (2006). Nicotine and smoker status moderate brain electric and mood activation induced by ketamine, an N-methyl-D-aspartate (NMDA) receptor antagonist. *Pharmacology Biochemistry and Behavior*, *85*, 228–242.
- Kocsis, B. (2012). Differential role of NR2A and NR2B subunits in N-methyl-D-aspartate receptor antagonist-induced aberrant cortical gamma oscillations. *Biological Psychiatry*, *71*, 987–995.
- Kometer, M., Pokorny, T., Seifritz, E., & Volleinweider, F. X. (2015). Psilocybin-induced spiritual experiences and insightfulness are associated with synchronization of neuronal oscillations. *Psychopharmacology (Berl)*, *232*, 3663–3676.
- Krijzer, F., Koopman, P., & Olivier, B. (1993). Classification of psychotropic drugs based on pharmaco-electrocorticographic studies in vigilance-controlled rats. *Neuropsychobiology*, *28*, 122–137.
- Kucewicz, M. T., Cimbalknik, J., Matsumoto, J. Y., Brinkmann, B. H., Bower, M. R., Vasoli, V., ... Worrell, G. A. (2014). High frequency oscillations are associated with cognitive processing in human recognition memory. *Brain*, *137*, 2231–2244.
- Kulikova, S. P., Tolmacheva, E. A., Anderson, P., Gaudias, J., Adams, B. E., Zheng, T., & Pinault, D. (2012). Opposite effects of ketamine and deep brain stimulation on rat thalamocortical information processing. *European Journal of Neuroscience*, *36*, 3407–3419.
- Lazarewicz, M. T., Ehrlichman, R. S., Maxwell, C. R., Gandal, M. J., Finkel, L. H., & Siegel, S. J. (2010). Ketamine modulates theta and gamma oscillations. *Journal of Cognitive Neuroscience*, *22*, 1452–1464.
- Leccese, A. P., Marquis, K. L., Mattia, A., & Moreton, J. E. (1986). The anticonvulsant and behavioral effects of phencyclidine and ketamine following chronic treatment in rats. *Behavioral Brain Research*, *22*, 257–264.
- Lee, J., Hudson, M. R., O'Brien, T. J., Nithianantharajah, J., & Jones, N. C. (2017). Local NMDA receptor hypofunction evokes generalized effects on gamma and high-frequency oscillations and behavior. *Neuroscience*, *358*, 124–136.
- Lee, D., Shtengel, G., Osborne, J. E., & Lee, A. K. (2014). Anesthetized-and awake-patched whole-cell recordings in freely moving rats using UV-cured collar-based electrode stabilization. *Nature Protocols*, *9*, 2784–2795.
- Lidierth, M. (2009). sigTOOL: A MATLAB-based environment for sharing laboratory-developed software to analyze biological signals. *Journal of Neuroscience Methods*, *178*, 188–196.
- Matulewicz, P., Kasicki, S., & Hunt, M. J. (2010). The effect of dopamine receptor blockade in the rodent nucleus accumbens on local field potential oscillations and motor activity in response to ketamine. *Brain Research*, *1366*, 226–232.
- Middleton, S., Jalics, J., Kispersky, T., Lebeau, F. E. N., Roopun, A. K., Kopell, N. J., ... Cunningham, M. O. (2008). NMDA receptor-dependent switching between different gamma rhythm-generating microcircuits in entorhinal cortex. *Proceedings of the National Academy of Sciences of the United States of America*, *105*, 18572–18577.
- Molina, L. A., Skelin, I., & Gruber, A. J. (2014). Acute NMDA receptor antagonism disrupts synchronization of action potential firing in rat prefrontal cortex. *PLoS ONE*, *9*, e85842.
- Muthukumaraswamy, S. D., Shaw, A. D., Jackson, L. E., Hall, J., Moran, R., & Saxena, N. (2015). Evidence that subanesthetic doses of ketamine cause sustained disruptions of NMDA and AMPA-mediated frontoparietal connectivity in humans. *Journal of Neuroscience*, *35*, 11694–11706.
- Nicolás, M. J., López-Azcárate, J., Valencia, M., Alegre, M., Pérez-Alcázar, M., Iriarte, J., & Artieda, J. (2011). Ketamine-induced oscillations in the motor circuit of the rat basal ganglia. *PLoS ONE*, *6*, e21814.
- Niell, C. M., & Stryker, M. P. (2010). Modulation of visual responses by behavioral state in mouse visual cortex. *Neuron*, *65*, 472–479.
- Noga, B. R., Sanchez, F. J., Villamil, L. M., O'Toole, C., Kasicki, S., Olszewski, M., ... Jordan, L. M. (2017). LFP oscillations in the mesencephalic locomotor region during voluntary locomotion. *Frontiers in Neural Circuits*, *11*, 34.
- Nottage, J. F., & Horder, J. (2015). State-of-the-art analysis of high-frequency (gamma range) electroencephalography in humans. *Neuropsychobiology*, *72*, 219–228.
- Nugent, A. C., Ballard, E. D., Gould, T. D., Park, L. T., Moaddel, R., Brutsche, N. E., & Zarate, C. A. (2018). Ketamine has distinct

- electrophysiological and behavioral effects in depressed and healthy subjects. *Molecular Psychiatry*, 1–13. <https://doi.org/10.1038/s41380-018-0028-2>
- Olszewski, M., Dolowa, W., Matulewicz, P., Kasicki, S., & Hunt, M. J. (2013). NMDA receptor antagonist-enhanced high frequency oscillations: Are they generated broadly or regionally specific? *European Neuropsychopharmacology*, 23, 1795–1805.
- Páleníček, T., Fujáková, M., Brunovský, M., Balfiková, M., Horáček, J., Gorman, I., ... Krajča, V. (2011). Electroencephalographic spectral and coherence analysis of ketamine in rats: Correlation with behavioral effects and pharmacokinetics. *Neuropsychobiology*, 63, 202–218.
- Pham, T. H., Defaix, C., Xu, X., Deng, S.-X., Fabresse, N., Alvarez, J.-C., ... Gardier, A. M. (2017). Common neurotransmission recruited in (R, S)-ketamine and (2R,6R)-hydroxynorketamine-induced sustained antidepressant-like effects. *Biological Psychiatry*, 84, e3–e6.
- Pinault, D. (2008). N-methyl d-aspartate receptor antagonists ketamine and MK-801 induce wake-related aberrant gamma oscillations in the rat neocortex. *Biological Psychiatry*, 63, 730–735.
- Powers, A. R., Gancsos, M. G., Finn, E. S., Morgan, P. T., & Corlett, P. R. (2015). Ketamine-induced hallucinations. *Psychopathology*, 48, 376–385.
- Réus, G. Z., Stringari, R. B., Ribeiro, K. F., Ferraro, A. K., Vitto, M. F., Cesconetto, P., ... Quevedo, J. (2011). Ketamine plus imipramine treatment induces antidepressant-like behavior and increases CREB and BDNF protein levels and PKA and PKC phosphorylation in rat brain. *Behavioral Brain Research*, 221, 166–171.
- Riba, J., Anderer, P., Morte, A., Urbano, G., Jané, F., Saletu, B., & Barbanoj, M. J. (2002). Topographic pharmaco-EEG mapping of the effects of the South American psychoactive beverage ayahuasca in healthy volunteers. *British Journal of Clinical Pharmacology*, 53, 613–628.
- Rivolta, D., Heidegger, T., Scheller, B., Sauer, A., Schaum, M., Birkner, K., ... Uhlhaas, P. J. (2015). Ketamine dysregulates the amplitude and connectivity of high-frequency oscillations in cortical-subcortical networks in humans: Evidence from resting-state magnetoencephalography-recordings. *Schizophrenia Bulletin*, 41, 1105–1114.
- Scheffzük, C., Kukushka, V. I., Vyssotski, A. L., Draguhn, A., Tort, A. B. L., & Brankač, J. (2013). Global slowing of network oscillations in mouse neocortex by diazepam. *Neuropharmacology*, 65, 123–133.
- Schmitt, U., & Hiemke, C. (1998). Combination of open field and elevated plus-maze: A suitable test battery to assess strain as well as treatment differences in rat behavior. *Progress in Neuro-Psychopharmacology & Biological Psychiatry*, 22, 1197–1215.
- Schultz, A., Schultz, B., Zachen, B., & Pichlmayr, I. (1990). Ketamineeffekte im elektroenzephalogramm—typische muster und spektraldarstellungen. *Anaesthesist*, 39, 222–225.
- Schwartz, M. S., Virden, S., & Scott, D. F. (1974). Effects of ketamine on the electroencephalograph. *Anaesthesia*, 29, 135–140.
- Schwarz, C., Hentschke, H., Butovas, S., Haiss, F., Stüttgen, M. C., Gerdjikov, T. V., ... Waiblinger, C. (2010). The head-fixed behaving rat—procedures and pitfalls. *Somatosensory and Motor Research*, 27, 131–148.
- Sebban, C., Tesolin-Decros, B., Ciprian-Ollivier, J., Perret, L., & Spedding, M. (2002). Effects of phencyclidine (PCP) and MK 801 on the EEGq in the prefrontal cortex of conscious rats; antagonism by clozapine, and antagonists of AMPA-, alpha(1)- and 5-HT(2A)-receptors. *British Journal of Pharmacology*, 135, 65–78.
- Shin, J., Kim, D., Bianchi, R., Wong, R. K. S., & Shin, H.-S. (2005). Genetic dissection of theta rhythm heterogeneity in mice. *Proceedings of the National Academy of Sciences of the United States of America*, 102, 18165–18170.
- Ślawińska, U., & Kasicki, S. (1998). The frequency of rat's hippocampal theta rhythm is related to the speed of locomotion. *Brain Research*, 796, 327–331.
- Slovik, M., Rosin, B., Moshel, S., Mitelman, R., Schechtman, E., Eitan, R., ... Bergman, H. (2017). Ketamine induced converged synchronous gamma oscillations in the cortico-basal ganglia network of nonhuman primates. *Journal of Neurophysiology*, 118, 917–931.
- Steele, A. D., Jackson, W. S., King, O. D., & Lindquist, S. (2007). The power of automated high-resolution behavior analysis revealed by its application to mouse models of Huntingtons and prion diseases. *Proceedings of the National Academy of Sciences of the United States of America*, 104, 1983–1988.
- van Dam, E. A., van der Harst, J. E., ter Braak, C. J. F., Tegelenbosch, R. A. J., Spruijt, B. M., & Noldus, L. P. J. J. (2013). An automated system for the recognition of various specific rat behaviours. *Journal of Neuroscience Methods*, 218, 214–224.
- van den Boom, B. J. G., Pavlidi, P., Wolf, C. J. H., Mooij, A. H., & Willuhn, I. (2017). Automated classification of self-grooming in mice using open-source software. *Journal of Neuroscience Methods*, 289, 48–56.
- van Lier, H., Drinkenburg, W. H. I. M., & Coenen, A. M. L. (2003). Strain differences in hippocampal EEG are related to strain differences in behaviour in rats. *Physiology & Behavior*, 78, 91–97.
- van Lier, H., Drinkenburg, W. H. I. M., van Eeten, Y. J. W., & Coenen, A. M. L. (2004). Effects of diazepam and zolpidem on EEG beta frequencies are behavior-specific in rats. *Neuropharmacology*, 47, 163–174.
- Tizabi, Y., Bhatti, B. H., Manaye, K. F., Das, J. R., & Akinfiresoye, L. (2012). Antidepressant-like effects of low ketamine dose is associated with increased hippocampal AMPA/NMDA receptor density ratio in female Wistar-Kyoto rats. *Neuroscience*, 213, 72–80.
- Vanderwolf, C. H. (1969). Hippocampal electrical activity and voluntary movement in the rat. *Electroencephalography and Clinical Neurophysiology*, 26, 407–418.
- Visser, S. A. G., Wolters, F. L. C., Gubbens-Stibbe, J. M., Tukker, E., van der Graaf, P. H., Peletier, L. A., & Danhof, M. (2003). Mechanism-based pharmacokinetic/pharmacodynamic modeling of the electroencephalogram effects of GABAA receptor modulators: In vitro-in vivo correlations. *Journal of Pharmacology and Experimental Therapeutics*, 304, 88–101.
- Wang, Z., Mirbozorgi, A., & Ghovanloo, M. (2015). Towards a kinect-based behavior recognition and analysis system for small animals. *2015 IEEE Biomedical Circuits and Systems Conference (BioCAS)*.
- Wood, J., Kim, Y., & Moghaddam, B. (2012). Disruption of prefrontal cortex large scale neuronal activity by different classes of psychotomimetic drugs. *Journal of Neuroscience*, 32, 3022–3031.
- Yamamoto, S., Ohba, H., Nishiyama, S., Harada, N., Kakiuchi, T., Tsukada, H., & Domino, E. F. (2013). Subanesthetic doses of ketamine transiently decrease serotonin transporter activity: A PET study in conscious monkeys. *Neuropsychopharmacology*, 38, 2666–2674.
- Zanos, P., Moaddel, R., Morris, P. J., Georgiou, P., Fischell, J., Elmer, G. I., ... Gould, T. D. (2016). NMDAR inhibition-independent antidepressant actions of ketamine metabolites. *Nature*, 533, 481–486.
- Zarringhalam, K., Ka, M., Kook, Y.-H., Terranova, J. I., Suh, Y., King, O. D., & Um, M. (2012). An open system for automatic home-cage behavioral analysis and its application to male and female mouse models of Huntington's disease. *Behavioral Brain Research*, 229, 216–225.

Zhang, Y., Yoshida, T., Katz, D. B., & Lisman, J. E. (2012). NMDAR antagonist action in thalamus imposes δ oscillations on the hippocampus. *Journal of Neurophysiology*, *107*, 3181–3189.

SUPPORTING INFORMATION

Additional supporting information may be found online in the Supporting Information section at the end of the article.

How to cite this article: Hansen IH, Agerskov C, Arvastson L, Bastlund JF, Sørensen HBD, Herrik KF. Pharmaco-electroencephalographic responses in the rat differ between active and inactive locomotor states. *Eur J Neurosci*. 2019;50:1948–1971. <https://doi.org/10.1111/ejn.14373>